Impacts of intracellular lipid mobilisation on endothelial dysfunction

Yu Huang

A thesis submitted in fulfilment of the requirements for the degree of

Master of Philosophy (Medicine)

Centenary Institute

Faculty of Medicine and Health

The University of Sydney

2023

Statement of Originality

This is to certify that the content of this thesis is the product of my own work and has not been submitted for any other degree or purpose. I certify that all the assistance received in preparing this thesis and sources have been acknowledged.

Yu Huang

June 2023

Abstract

Lipid metabolism and transport are important for the development of cardiovascular diseases (CVD). Oxysterol-binding related proteins-2 (ORP2) is the only known lipid transporter to transport cholesterol on the plasma membrane (PM). Knockdown of ORP2 in human umbilical vein endothelial cells (HUVEC) shows downregulation of pro-inflammatory signals under endothelial activation induced by TNF-α and turbulent flow. Knockdown of ORP2 can also disrupt the endothelial recruitment of monocytes. However, deficiency of ORP2 does not alter the expression of lipid rafts structural proteins Flotllin-1 and Caveolae-1.

Additionally, expression of ORP2 is found to be upregulated in endothelial senescence. Knockdown of ORP2 after oxidative stress stimulation can efficiently block the progress of senescence. On the other hand, lipid profiling of hydrogen peroxide (H_2O_2) induced endothelial senescence was conducted with a combination of targeted and untargeted lipidomics analysis. A total of 336 lipid species have been analysed so far in this study. Alterations of lipids during the progression of senescence were found in classes of sphingolipid, glycerophospholipid, free fatty acid and cholesterol.

Overall, this thesis provides evidence of the importance of ORP2 in CVD and the endothelial senescent lipidome profile. These results give insights for research on cardiovascular disease and cellular senescence mechanisms. Future work will expand lipid profiling to include more lipid species in this study and testify to the function of ORP2 in animal models and subcellular structure.

Acknowledgements

It has been a long journey for my study for this MPhil degree, and I have received so much help in research and daily life from all those kind people. The word cannot nearly express my gratitude.

I would very much appreciate my supervisor, Dr. Yanfei (Jacob) Qi. Dr. Qi offered my extraordinary supervision in research. He has taught me the integrity and methods to perform proper research. He showed me the way to enter the field of lipid study.

I also much appreciate my co-supervisor, Prof. Jennifer Gamble, and her research group, who support and inspire me in vascular biology studies.

I would like to thank the members of Qi's lab. Dr. Long Hoa Chung offered me much help in lipidomics studies. I would especially like to thank Xingxing Han for helping me perform RT-qPCR in senescent HUVECs.

I would like to thank the collaborating research group, Don's lab, for offering me advice on lipid analysis. I would also thank other researchers and research support teams at Centenary Institute and Charles Perkins Centre—especially the support I got offered from researchers working at Sydney Masspect and Sydney Microscopy.

The research of this thesis is funded by the National Health Medical Research Council, Australia (NHMRC).

Finally, I would appreciate my family's and friends' support.

Abbreviations

Amphotericin B	AmB
ADP-ribosylation factor	ARF
p53-cyclin-dependent kinase inhibitor 1A	CDKN1A, p21
p53-cyclin-dependent kinase inhibitor 1B	CDKN1B, p16
Cholesterol esters	CE
Ceramide	Cer
Cyclic guanosine monophosphate	cGMP
Cholesterol	Chol
Cyclooxygenase	COX
Cardiovascular diseases	CVD
Diacylglycerol	DG or DAG
Dulbecco’s modified Eagle medium	DMEM
Endothelial cells	EC
Endothelium-dependent dilatation	EDD
Endothelial NO synthase	eNOS
Fetal bovine serum	FBS

Free fatty acid	FFA
Glycerophospholipid	GPL
Guanosine triphosphate	GTP
Hexosylceramide	HexCer
Human umbilical vein endothelial cell	HUVEC
Intercellular adhesion molecule 1	ICAM1
Interleukin-1	IL-1
Intraluminal vesicles	ILV
Lysosomal acid lipase	LAL
Liquid chromatography	LC
Late endosomes	LE
Lysosome	Lys
Monocyte chemoattractant protein-1	MCP-1
Membrane contact sites	MCS
Monoacylglycerol	MG or MAG
Mass spectrometry	MS
Multivesicular bodies	MVB

NLR-family pyrin domain-containing protein 3	NLRP3
Nitric oxide	NO
Niemann-Pick C	NPC
OSBP homology	OH
OSBP-related lipid-binding domain	ORD
Oxysterol-binding proteins	OSBP
Oxysterol-binding related proteins	OSBPL or ORP
Oxidised low-density lipoprotein	ox-LDL
Phospho-p65	p-p65
Phosphatidylcholine	PC
Phosphatidylethanolamine	PE
Prostacyclin	PGI2
Pleckstrin homology domain	PH domain
Phosphatidylinositol-4,5-bisphosphate	$PI(4,5)P_2$
Phosphatidylinositol 4-phosphate	PI4P
Phosphatidylinositol phosphate	PIP
Protein kinase G	PKG

Plasma membrane	PM
Peroxisomal proliferator-activated receptor	PPAR
Reactive oxygen species	ROS
Senescence-associated β-galactosidase	SA-β-gal
Senescence-associated secretory phenotypes	SASP
Short hairpin RNA	shRNA
Small interfering RNA	siRNA
Sphingolipid	SL
Sphingomyelin	SM
Smooth muscle cell(s)	SMC(s)
Total p65	t-P65
Transendothelial migration	TEM
Triacylglycerol	TG or TAG
Trans-Golgi network	TGN
Tumour necrosis factor	TNF
VAMP-associated proteins	VAP
Vascular cell adhesion adhesion molecule 1	VCAM-1

Vascular endothelial growth factor receptor 2	VEGFR2

Table of Content

Chapter 1 Literature Review

1.1 Vascular Endothelium

The endothelium is the simple monolayer made of endothelial cells, the inner layer of blood vessels carrying blood flow. Researchers used to believe that the endothelium was only the “wrapper” inside blood vessels with a simple function of selective permeability with water, electrolytes and some other small products [1]. However, this simple monolayer of endothelial cells affords complicated functions. In response to chemical and biological signals, the endothelial cells generate various factors, such as nitric oxide (NO) and prostacyclin (PGI_2), whereby they regulate immune cell adhesion, the proliferation of smooth muscle cells, and vessel inflammation.

1.1.1 Endothelial Homeostasis

While considering a simple monolayer of the endothelium, the endothelium can react to both physical and chemical stress from metabolic waste and other toxic contents carried with blood flow to keep homeostasis in the endothelium and blood vessels. These are accomplished by the diverse array of cellular factors, such as nitric oxide and PGI2, to govern vascular tone, cellular adhesion, anti-atherosclerosis, proliferation of smooth muscle cells (SMCs) and inflammation at vessel walls [2, 3].

One of the crucial regulators, Nitric oxide, is produced in endothelial cells as an endothelium-derived relaxing factor through the action of endothelial NO synthase (eNOS) using L-arginine as the substrate [4, 5]. This synthesis also requires the presence of tetrahydrobiopterin and some other cofactors. Once NO is produced in the endothelial cells, the gaseous NO molecules diffuse into the smooth muscle cells (SMC) layer to activate guanylate cyclase. Guanylate cyclase, in turn, facilitates the conversion of guanosine triphosphate (GTP) into cyclic guanosine monophosphate(cGMP), which subsequently activates protein kinase G (PKG) [6].

Through the activation of cGMP/PKG, numerous Ca^{2+} channel proteins on the plasma membrane are phosphorylated, resulting in the decrease of cellular Ca^{2+} concentration and enhanced vascular relaxation [7].

Nitric oxide achieves its diverse functions by engaging the S-nitrosylation, leading to the deactivation of specific proteins [8], including NFκB and cell cycle-related proteins [9]. S-nitrosylation is recognised as a reversible modification similar to phosphorylation [10]. In the cardiovascular system, NO-mediated S-nitrosylation could result in various regulations of apoptosis [11], SMC proliferation [12], exocytosis [13] and the activity of ion channel proteins and blood flow.

In vivo, shear stress stands out as a major regulator that activates eNOS, facilitating organ perfusion adjustments in response to changes in cardiac output [14]. Besides, eNOS can also be triggered by other signalling molecules such as bradykinin, adenosine, and endothelial growth factors [15].

Another key regulator in terms of endothelial homeostasis, prostacyclin (PGI_2), is produced from arachidonic acid (C20:4), an ω-3 polyunsaturated fatty acid. This synthesis requires catalysing with cyclooxygenase (COX), which makes up another endothelium-dependent vasodilator [16]. Apart from the role of the vasodilator, PGI_2 also contributes to a list of other functions such as antiproliferation, antithrombotic, anti-inflammatory and antimitogenic [17].

1.1.2 Endothelial Dysfunction and Vascular Inflammation

Endothelial dysfunction, or endothelial activation, is a procedure in which endothelium is transited from the “stop phase” to the “action phase”. This shift disrupts the balance and homeostasis of the endothelium, which ultimately contributes to the development of various vascular diseases.

1.1.2.1 Mechanism of Endothelial Activation

In the healthy condition of the endothelium, complex IV in mitochondria, transcription factor NFκB (p50/p65) and some other key regulator molecules were deactivated by the S-nitrosylation conducted with the nitro oxide synthesised from eNOS. However, during endothelium activation, these NO-mediated deactivated signalling pathways can be triggered by reactive oxygen species (ROS) [18, 19]. Consequently, endothelium activation can be found as a physiological phenotype in inflammatory contexts or as a pathophysiological phenotype in cardiovascular diseases.

Interestingly, in endothelial activation, the ROS are generated from eNOS, which was the former “housekeeper” of endothelial homeostasis. This change occurs due to the uncoupling of eNOS dimer[20]. There are two distinct pathways through which eNOS mediates the generation of ROS. One produces superoxide when losing tetrahydrobiopterin as the core cofactor, and another produces hydrogen peroxide when L-arginine as the substrate is dysfunctional [5]. Hydrogen peroxide that is converted from ROS in the presence of superoxide dismutase can be rapidly released within endothelial cells and perform reactions with cysteine sites of multiple proteins to activate the NO-mediated deactivations [19]. These regulations can result in various changes, including phosphorylation of transcription factors, induction of

chromatin remodelling and activation of proteinase. Therefore, eNOS is critical in the regulation of endothelium homeostasis and activation with its bifunctional synthesis of both nitro oxide and hydrogen peroxide.

In the human body, endothelial activation is part of the host defence system, which is the consequence of infection and injury.

1.1.2.2 Phenotypes of Endothelium Activation

The presence of endothelium in vascular acute inflammation acting was first discovered in post-capillary venules in 1965 [21, 22]. Classic inflammatory mediators such as histamine can influence vascular permeability, tone, and diapedesis of immune cells. This form of endothelium activation, named “Type I activation” [23], is a self-restricted action. Normally, Type 1 activation is not supposed to induce continuous morphological or functional changes in the endothelium or blood vessels. However, when endothelial cells are exposed to certain pathogenic products, lipoproteins, such as oxidised low-density lipoprotein (ox-LDL), or cytokines, such as tumour necrosis factor (TNF) and interleukin-1 (IL-1) [24], they undergo “Type II activation” [23, 25]. Type II activation typically involves the activation of NFκB, which in turn leads to the activation of specific proteins that exert further pathological and physiological effects. In vitro studies using cytokines such as TNF-α reveal the upregulation of various signalling markers. These include inducible adhesion molecules that promote the leukocyte-endothelial adhesion, such as ELAM-1 (E-selectin), ICAM-1 (CD54) and VCAM-1 (CD106) [26]; secreted chemokines, such as monocyte chemoattractant protein-1 (MCP-1) [27] and IL-8 [28], as well as procoagulant molecules. The expressions of these proteins facilitate the transition of endothelial cells to a mildly pro-inflammatory phenotype.

This pro-inflammatory activation can also be found in vivo at the sites of the vascular inflammation [29]. This phenotype is the entrance to understanding the role of the endothelium in vascular inflammatory responses and the genesis of cardiovascular diseases (CVD).

NFκB occupies a central role in terms of the regulation of pro-inflammatory processes during endothelial activation. The pathophysiologic consequences of endothelial dysfunction are predominantly associated with the NFκB signalling pathway in the aorta endothelium [30]. NFκB is in charge of expressions of various endothelial adhesion molecules in atherogenesis, such as ICAM-1 [31], E-selectin (ELAM-1) [32] and VCAM-1 [33, 34]. As a transcription factor, NFκB is essential for endothelium to respond to shear stress via its capability to bind onto certain flow-sensitive genes' promoters on specific binding sites. Interestingly, NFκB tends to enhance the activation at athero-prone sites in response to certain stimuli. Recent research also indicated that NFκB is capable of modifying the structure of endothelial cell chromatins, as epigenetic changes, by inducing super-enhancer complexes [35].

Adhesion molecules serve as critical regulators governing inflammatory actions. These molecules not only facilitate cell-cell interaction but also establish the interaction between the cytoskeleton and various adaptor proteins, thereby initiating further intracellular signalling [36, 37].

The discovery of the adhesion molecules commenced with VCAM-1 [38], as it is a strong and sustained signal in the endothelium. Increased expression of VCAM-1 has been observed in humans [39] and in mice models of hypercholesterolemia induced by high cholesterol diets [40] or gene mutation of ApoE deficiency [34]. On the other hand, ICAM-1 exhibits relatively low basal expression levels in both

endothelial and immune cells. ICAM-1 has been well-studied for its involvement in leukocyte transendothelial migration (TEM), by facilitating the adhesion of leukocytes to endothelial cells and subsequent crossing of the endothelium monolayer [41]. Another critical regulator of TEM under endothelial activation, E-selectin, is exclusively present on the surface of endothelial cells. E-selectin is capable of directly promoting neutrophil and monocyte activity [42] and recruiting those immune cells onto activated endothelium [43]. Importantly, the soluble isoforms of VCAM-1 [44], ICAM-1[45] and E-selectin[45] can be detected in circulating blood, making blood concentrations of these adhesion molecules efficient markers for clinical diagnosis of atherosclerotic severity.

Another critical link between endothelial activation and atherogenesis is the generation of chemokines from activated endothelial cells and neighbouring smooth muscle cells. These chemokines trigger both paracrine and autocrine signalling pathways, promoting the adhesion of immune cells, such as T-lymphocytes, leukocytes and macrophages [46]. Through the cooperation of signalling molecules and immune cells, a complex inflammation network is established within vascular atherosclerosis lesions, regulating both local and systemic vascular inflammation [47].

In addition to the activation of NFκB, endothelium activation could also trigger the activation of NLR-family pyrin domain-containing protein 3 (NLRP3) inflammasome [48]. The NLRP3 inflammasome, a multimeric protein complex that assembles various cytosolic proteins, triggers the cleavage of pro-interleukin-1β (IL-1β) and pro-IL-18. This activation relies on the activation of the active form caspase-1 from pro-caspase-1 [49]. Recent research demonstrated the role of NLRP3 inflammasome

activation in driving pyroptosis [50, 51], an inflammatory programmed cell-intrinsic death, which has been considered a potential cause of endothelial cell death.

1.1.2.3 Diseases and Vascular Inflammation

Pathologically, a long list of acute and chronic inflammatory diseases has been proven associated with endothelial dysfunction [52], which includes those chronic diseases like rheumatoid arthritis [53, 54], systemic sclerosis [55], and those acute inflammatory diseases such as Kawasaki disease [56], severe sepsis [57].

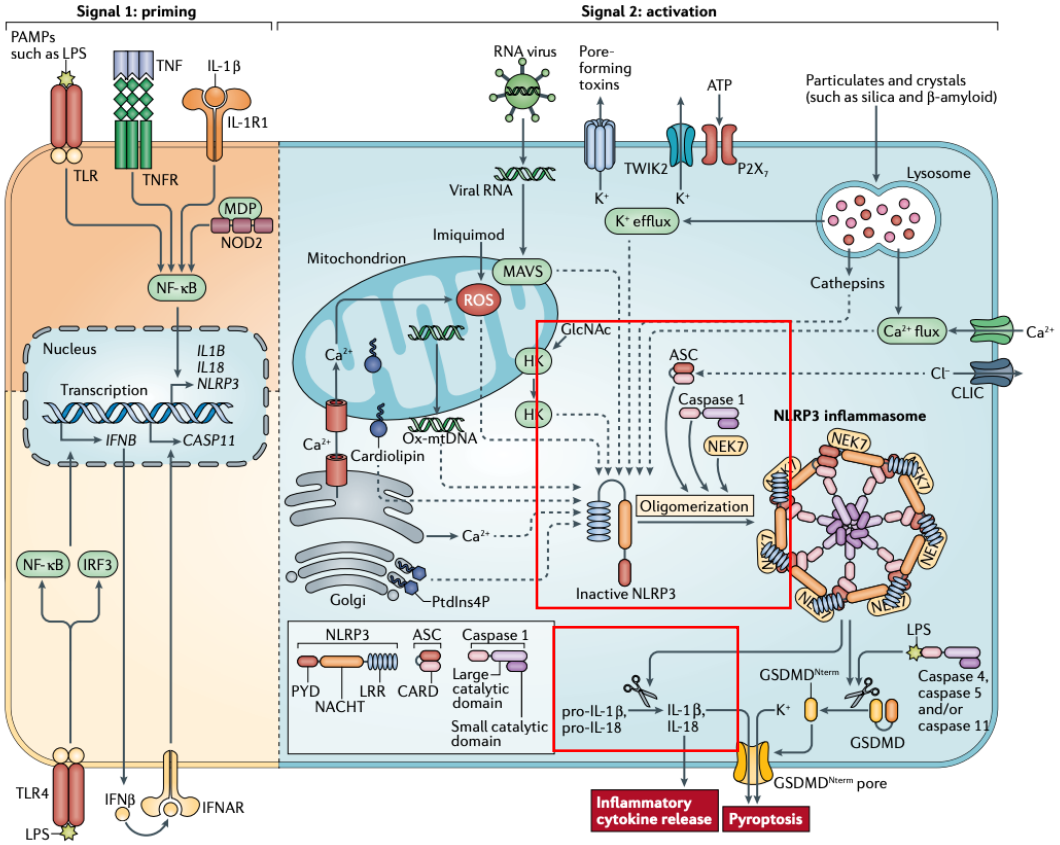

Figure 1-1. Activation and molecule recruitment of NLRP3 inflammasomes.

Revised from [58].

1.1.3 Endothelial Senescence

Cellular senescence refers to a state of non-proliferation observed in cells upon exposure to various stressors. The concept of senescence was firstly described in the 1960s [59].

1.1.3.1 Mechanisms of Endothelium Senescence

Essentially, endothelial senescence is an irreversible proliferation arrest triggered by oxidative stress, replicative stress or inflammation [60]. In healthy bodies, senescence serves as a mechanism for clearing damaged cells. However, in pathological conditions, the homeostasis of senescence and clearance is disrupted under continuous damage or immune dysfunction, therefore leading to the accumulation of senescent cells [60, 61]. The accumulation of senescent cells within endothelium can lead to a range of cardiovascular dysfunctions and diseases, such as disrupted endothelium-dependent dilatation (EDD) [62], impaired angiogenesis [63], disordered endothelium permeability [64], hypertension [65], atherosclerosis [66, 67] and heart failure [68]. Consequently, it is crucial to understand the regulation and the dysregulation of EC senescence to lead to therapeutic development for cardiovascular disease.

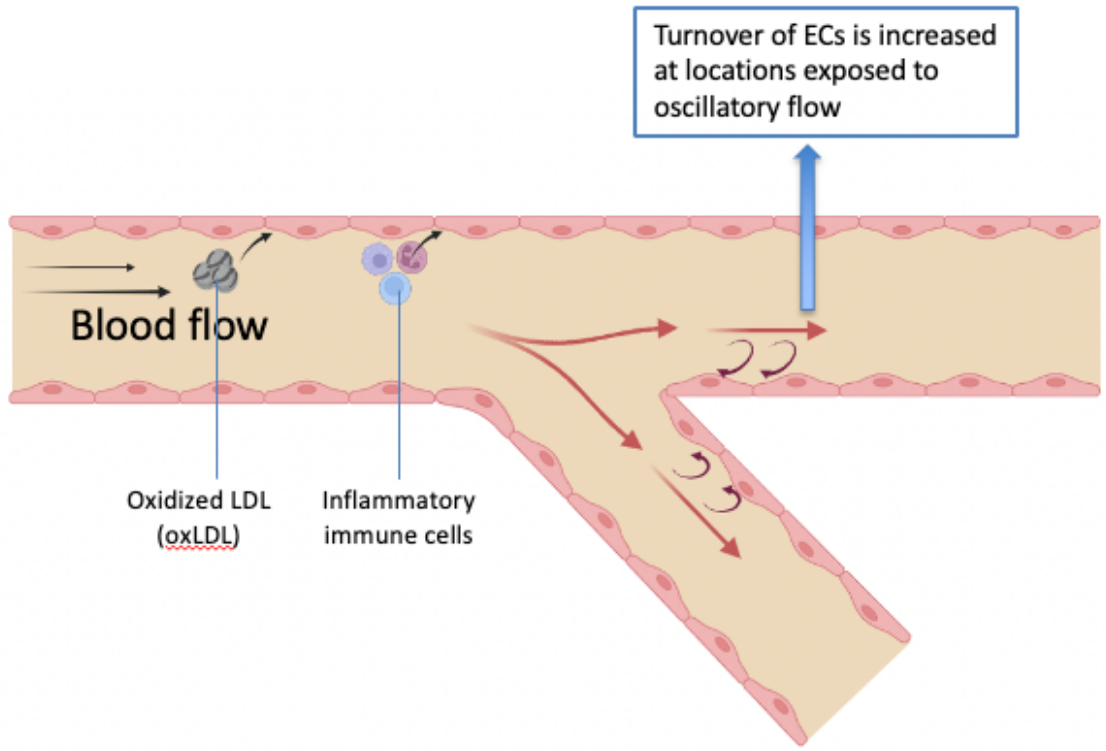

Figure 1-2. Causes of endothelium senescence.

Immune cells, oxidised low-density lipoprotein (oxLDL) and other metabolic production carrying with blood flow contribute to oxidative and inflammatory stress; meanwhile, oscillatory blood flow that occurs in the brunch of blood vessels promotes the proliferation of endothelial cells and therefore causes repetitive stress.

1.1.3.2 Phenotypes of Senescence

Cellular senescence with the stress of aging and oxidisation can limit the capacity of repairing in surrounding endothelial cells and generate pro-inflammatory signals, acting on the region of vessels and causing vascular inflammation. Endothelial microparticles as the key circulating markers generated from activated, apoptotic and even functional endothelial cells during this damage can be found increasing in cardiovascular or peripheral atherosclerosis and other inflammatory circumstances such as systemic lupus erythematosus and rheumatoid arthritis [69, 70].

In EC senescence, morphological changes occur, characterised by a flattened and enlarged shape compared to healthy ECs. Consequently, senescent cells exhibit a “lazy” response to laminar shear stress and mechanistically disrupt alignment to the blood flow [71].

In normal cells, the cell cycle is tightly regulated by tumour suppressor pathways. However, in senescent cells, there is a notable upregulation of two key tumour suppressor pathways, which include p53-cyclin-dependent kinase inhibitor 1A (CDKN1A, p21) and retinoblastoma-associated protein (CDKN1B, p16) [60, 72]. P21 and p16 can both be used as reliable markers for detecting senescence, as they are activated differently depending on cell type, stressor and stage of senescence [73].

Apart from p21 and p16, another senescent marker was introduced as lysosomal senescence-associated β-galactosidase (SA-β-gal), which was found to have a high level of activity in senescent cells [74]. It is highly recommended to combine multiple markers together to detect senescent cells accurately [75].

In addition to detection markers, senescent cells are also characterised by their senescence-associated secretory phenotypes (SASP) [76]. The classic SASP is represented by the secretion of a combination of inflammatory chemokines, growth factors, cytokines, and ROS originating from senescent cells [77]. The production of ROS is suggested to be associated with impaired mitochondrial respiration and the subsequent accumulation of superoxide production [78]. The secretory ROS could further enhance SASP and damage endothelial function.

Typically, senescent ECs are observed to be pro-inflammatory. In EC senescence, activation of NFκB was found [79]. Senescent EC also produces a large range of chemokines and cytokines such as IL-1β [80], IL-8 and various adhesion molecules [81]. However, an anti-inflammatory phenotype is also reported in EC senescence horizontally existing with pro-inflammatory effects [82].

1.2 Intracellular Cholesterol and ORP Family Proteins

1.2.1 Intracellular Cholesterol

High cholesterol levels in the bloodstream have been extensively acknowledged as a risk factor for atherosclerosis in clinical practice. Absorption of cellular cholesterol is through both internal synthesis and external receptor-mediated lipoprotein uptake. Cholesterol plays a vital role in maintaining the functionality of cellular membranes and can regulate the permeability of cell membranes by increasing accumulating phospholipids to restrict molecule transmembrane actions. Cholesterol is essential for organelle membranes. However, its distribution highly varies among different organelles and with a strictly regulated total intracellular amount [83, 84].

1.2.2 Intracellular Cholesterol Transport

Cholesterol is an important lipid component of cellular membrane structure and functions; particularly, cholesterol predominantly localises on plasma membrane (PM) and interacts with other neighbouring lipids to regulate the biophysical property of PM and achieve essential functions such as cell-pathogens interactions and signal transduction. [85-88].

The cellular supply of cholesterol requires endogenous synthesis and uptake from the external environment. Endogenous cholesterol is synthesised in the ER. Cholesterol esters (CE) in lipoproteins are initially hydrolysed by lysosomal acid lipase (LAL) and released as free cholesterol for endocytosing. This process occurs

in late endocytic organelles, where free cholesterol is subsequently transported into the late endosomes (LE) and lysosomes (Lys) [89]. This LE/Lys transportation of cholesterol is regulated by Niemann-Pick C (NPC) proteins, including NPC1 and NPC2. NPC1 is a limiting membrane integral protein, while NPC2 is a luminal protein [90]. This process involves NPC2 delivering cholesterol to the NPC1 localised inside the targeted membrane. Once cholesterol reaches LE/Lys, it undergoes further transport and is eventually delivered to the PM. Excess cholesterol is subsequently delivered back to the ER, where cholesterol gets esterified and stored [91].

In addition to the LE/Lys transport of cholesterol, cholesterol can also be redirected back to ER directly [90] or via peroxisomes [92], which occurs on specific membrane contact sites (MCS) of these organelles [93]. There are different types of contact between ER and LE, such as contact associated with epidermal growth factor receptor (EGFR) and contact associated with VAMP-associated proteins (VAP) [94]. MCS plays a crucial role in regulating cholesterol homeostasis and facilitating inter-organelle communication.

When cells experience a shortage of external cholesterol, cholesterol endogenous synthesis that primarily happens in ER is enhanced to fulfil cellular demand for essential cholesterol. In this case, apart from regular cholesterol transport, there is a requirement for cholesterol to be transported from the ER to the endosome that typically acquires cholesterol from PM through endocytosing. This intracellular cholesterol source is crucial for the formation of cholesterol-rich intraluminal vesicles (ILV) within multivesicular bodies (MVB)/LE, which is an essential step in the endosome maturation and expansion [95]. The presence of cholesterol transport

within these intraluminal vesicles contributes to the overall dynamics and functionality of the endosomal system.

The transport of cholesterol within LE/ involves the association of various proteins. One important group of proteins are Rab GTPases, which regulate endomembrane compartments' maturation and vesicular trafficking to monitor the cholesterol transport associated with LE/Lys [96]. One example of GTPases is Rab7 GTPase, a regulator of cholesterol transport and MCS [97, 98].

1.2.3 Intracellular Cholesterol and Cardiovascular Diseases

Intracellular cholesterol may be implicated in various aspects of cardiovascular disease. Cholesterol plays a pivotal role as a crucial component within lipid rafts on the plasma membrane, which, in turn, can transmit inflammatory signals, particularly in response to stimuli like TNF [99, 100]. Additionally, cholesterol serves as a critical constituent in the inner mitochondrial membrane, where the regulation of inner membrane permeability and fluidity heavily depends on lipid composition due to the lack of porins [101, 102]. The accumulation of cholesterol in the inner mitochondrial membrane can significantly impact mitochondrial function, leading to mitochondrial dysfunction and an elevation in the release of reactive oxygen species (ROS) [102, 103]. Moreover, cholesterol crystal formation occurs within lysosomes, with a notable occurrence in macrophages [104]. The accumulation of cholesterol crystals in lysosomes can expedite the activation of the NLRP3 inflammasome [105]. Given the pro-inflammatory and ROS-inducing properties of cellular cholesterol, investigating cellular cholesterol emerges as a valuable focal point for studying cardiovascular diseases.

1.2.3 ORP Family

Oxysterol-binding proteins (OSBP) and Oxysterol-binding related proteins (OSBPL or ORP) constitute one of the largest intracellular lipid transfer protein groups that play a crucial role in intracellular lipid transport and homeostasis. ORPs are characterised by a C-terminal sterol-binding OSBP homology (OH) domain (Fig. 1-3). The function of ORP proteins is to localise and transfer lipids across MCS [106, 107]. ORP family members are characterised by their β-barrel-like OSBP-related lipid-binding domain (ORD) and possess the unique ability of "dual membrane targeting" [89]. Some ORPs have been testified as they can transfer lipids in opposite directions over different MCS [108-112]. The ORP family contains 12 proteins in mammals, with six of them having been proven involved in cholesterol transport. These includes OSBP, ORP1s, ORP1L, ORP2, ORP5 and ORP6 [89]. The collaboration of these ORP family proteins contributes to intracellular cholesterol traffic and homeostasis.

Figure 1-3. Structural organisation of the human ORP family proteins.

Revised from [113].

OSBP is the founding member of the ORP protein family and possesses distinct targeting abilities with its two phenylalanine residues in the acidic tract (FFAT). This FFAT motif enables OSBP to localise to the ER. Additionally, OSBP can target the trans-Golgi network (TGN) with its pleckstrin homology (PH) domain, which binds to phosphatidylinositol 4-phosphate (PI4P) and the small ADP-ribosylation factor (ARF) GTPases. The function of OSBP as a cholesterol transporter was firstly discovered as mediating bidirectional cholesterol-PI4P exchange in ER-TGN contact sites [109].

ORP1 exists in two variants: ORP1s (short) and ORP1L (long) [89]. Both of the variants contain an ORD domain, and ORP1L contains an additional FFAT domain (to target ER with VAP) and three ankyrin repeats close to the N-terminus [114]. The ankyrin repeats enable ORP1L to target LE by interacting with LE small GTPase Rab7 [98]. The interaction between ORP1L's FFAT domain and VAP proteins is sensitive to sterol levels and plays a role in regulating the positioning of LE [115]. Additionally, ORP1L can lead to contact between ER and autophagosome, which results in autophagy regulation.

ORP5 is anchored in ER membranes to interact with NPC1 on MCS and can conduct the removal of cholesterol on the LE/Lys-limiting membrane [116]. Besides, OORP5 has been implicated in the exchange of phosphatidylserine (PS) and phosphoinositide (PIP) at the ER-PM contacts [110, 117].

ORP2 is a cytosolic lipid transport protein [118]. ORP2’s function was initially demonstrated through overexpression studies, which showed that overexpression of ORP2 can enhance cellular cholesterol efflux and facilitate the transport of

endogenously synthesised cholesterol onto PM [118, 119]. ORP2 can bind and deliver oxysterols, cholesterol and phosphatidylinositol-4,5-bisphosphate ($PI(4,5)P_2$) [120-122]. Recent research suggested that ORP2 conducts a bidirectional transport of cholesterol between ER and plasma membrane [121]. After the knockdown of ORP2, hepatocytes exhibited a downregulation of cellular adhesion, proliferation, and cellular metabolism, such as glucose uptake, Triglyceride synthesis and storage, as well as AKT signalling [123, 124].

It has been well demonstrated that ORP2 facilitates intracellular cholesterol transport onto PM. Interestingly, ORP2 appears to be the only member of the ORP family that can drive this PM-directional cholesterol transport [121, 122]. Unlike other ORPs, ORP2 is a short version of ORP, which has an FFAT domain but lacks the N-terminal PH-domain (Fig. 1-3). ORP2 has also been observed participating in MCS between the ER and lipid droplets [125]. However, its function in this MCS is associated with TG synthesis rather than cholesterol-phosphatidylinositol phosphates (PIPs) exchange activity [120, 123, 126].

1.2.4 ORP2 in Vascular Biology

While ORP2 has been reported to play important roles in neurotransmitter [125], preadipocytes [127], and hearing function [128], another recent research firstly involved ORP2 into vascular biology studies [129]. ORP2 knockdown has been conducted in the human umbilical vein endothelial cells (HUVECs) [129]. This study revealed an increase of $PI(4,5)P_2$ in the PM. In ORP2 lentiviral knockdown HUVECs, a decrease in angiogenesis-related signals such as Vascular endothelial growth factor receptor 2 (VEGFR2), Akt, eNOS and Notch was observed. Besides, the proliferation viability and migration of ORP2-KD HUVECs were also reduced.

Furthermore, the expression of junction proteins such as VE-cadherin was also decreased.

1.3 Lipidomics for Metabolic Study

Lipids are a class of hydrophobic compounds that are essential for cellular structures and functions. Numerous lipid species are under regulation of a complex of metabolic network, which can respond to physiological and pathologic environment alterations. Lipidome is identified as the summarisation of cellular total lipid content [130].

1.3.1 Introduction of Lipids

The classification of lipids proposed by LIPID MAPS[131] classifies lipids into 8 lipid classes with additional subclasses. Five of lipid classes are considered essential in most of eukaryotes including sphingolipids (SLs), glycerophospholipids (GPLs), sterols, glycerolipids and free fatty acids (FFA).

Sphingolipids are crucial components of cellular membrane structure and are characterised by a long-chain sphingoid base. The biosynthesis of sphingolipids starts with the condensation of serine and palmitoyl-CoA with serine palmitoyltransferase, resulting in the formation of sphinganine. Sphinganine is then further modified, bypassing dihydroceramides, to convert to ceramide, which serves as the centre of sphingolipid metabolism. Ceramides (Cer) can be degraded to sphingosine and phosphorylated to sphingosine-1-phosphate (S1P) and, therefore, further degraded to non-sphingolipid compounds. On the other hand, after further

modification in ER or Golgi, ceramide can also be converted to complex sphingolipids, such as sphingomyelin (SM) and hexosylceramide (HexCer) [132, 133].

Glycerophospholipids are the main class of lipids that construct cellular membranes. GPLs are characterised by at least one O-acyl, O-alkyl or O-alk-1-enyl residue connected to glycerol with a phosphate head group. GPLs are further divided into subclasses by different modifications of phosphate head groups, such as phosphatidylcholine (PC) and phosphatidylethanolamine (PE) (Fig. 1-4).

The biosynthesis of glycerophospholipids strictly involves the remodelling of fatty acyl chains, which can occur either directly via the catalysis of transacylase or successively via the catalysis of fatty acyl hydrolysis and acyltransferase [134]. The de novo biosynthesis of ether-linked GPLs occurs in the peroxisome [135], whereas the synthesis of acyl-GPLs occurs in the ER [136]. Ether-linked GPLs are predominantly found in the subclasses of PC and PE [137]. The composition of GPL affects membranal functions of fusion, fission and molecule transport [138].

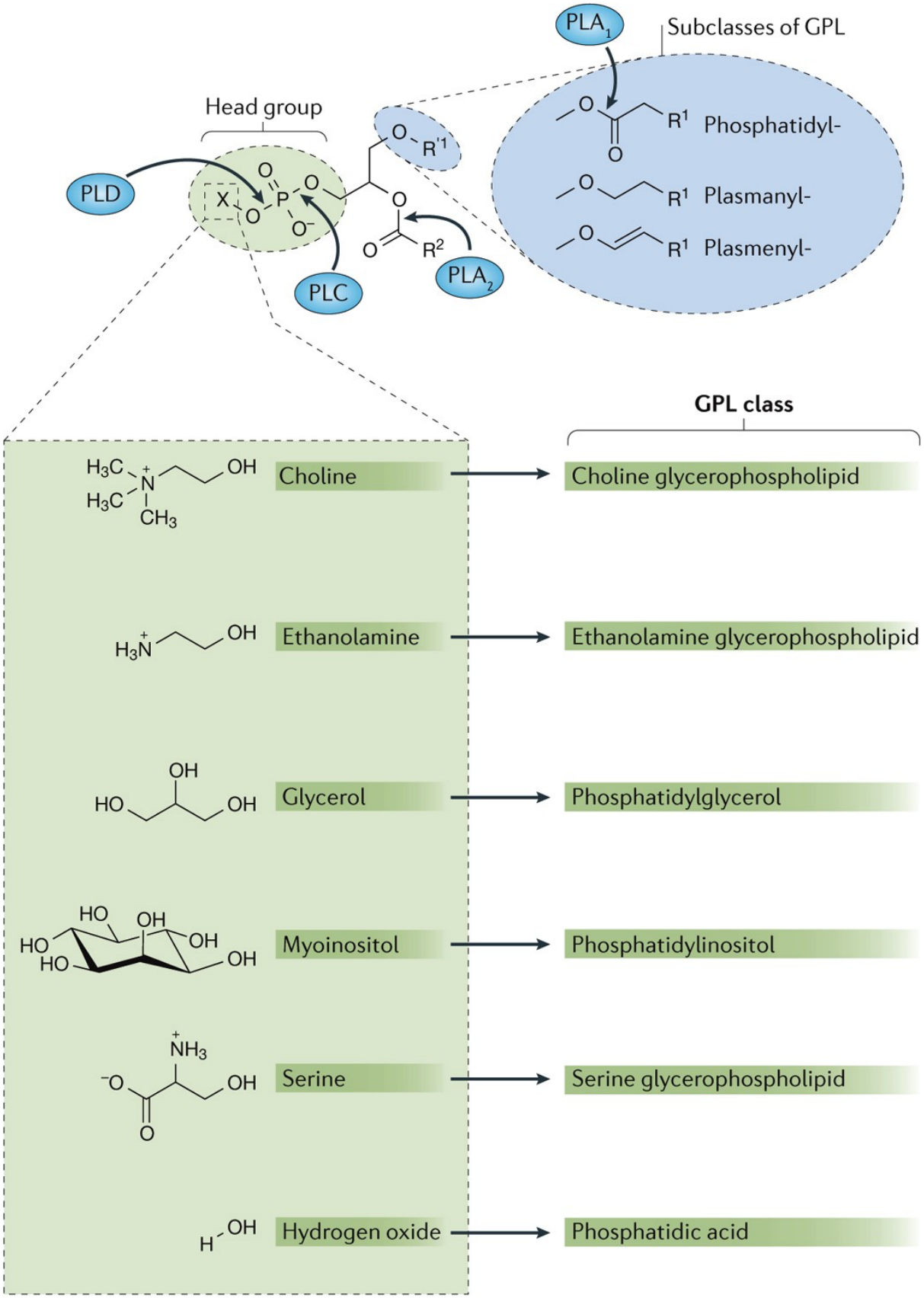

Figure 1-4. Structure of glycerophospholipids.

Revised from [139]

Glycerolipids typically include triacylglycerol (TG or TAG), diacylglycerol (DG or DAG), and monoacylglycerol (MG or MAG). TG is one of the major ways for cells to store energy; however, the accumulation of TG tends to be a marker of lipotoxicity and is related to insulin resistance [140]. Cellular TG storage occurs in the lipid droplets, which is a kind of organelle made of glycerophospholipid monolayer [141-143]. The biosynthesis of triglycerides (TG) occurs through the condensation of DG and acyl-CoA under the catalysis of diglyceride acyltransferase, which can be reversed with lipase. The biogenesis of DG is divided into two different pathways. One is from the dephosphorylation of phosphatidic acid, and the other way is from the reacylation of MG. Interestingly, the formation of DG can occur in different cellular locations, including the PM and the ER. In these locations, DG serves distinct functions related to its role as a signalling molecule and as the substrate for TG synthesis, respectively [144]. Moreover, MG has recently been reported to be associated with cellular signalling, such as peroxisomal proliferator-activated receptors (PPAR) [145].

Fatty acids are fundamental constructing materials of all lipids. The structure and composition of fatty acids tightly influence lipid metabolism. Different compositions of fatty acyl chains in lipids can lead to modified biofunction of lipids, such as alteration of membrane curvature and other biophysical properties. The biosynthesis of fatty acids begins with the condensation of multiple acetyl-CoAs and malonyl-CoA, resulting in the formation of palmitic acid C16:0. C16:0 will be further modified by desaturation, elongation and hydrolysis to form other fatty acid species. Remarkably,

different desaturations of fatty acids result in isomers with C-C double bonds located at different positions.

1.3.2 Lipidomic Analysis.

The metabolism of the lipidome is highly dynamic and responsive to changes in the cellular environment, making it important to capture lipid alterations for health research purposes. However, measuring and tracking lipids using traditional biological experimental methods is challenging due to their hydrophobic nature and the presence of isomers within lipid classes and subclasses. Lipidomics offers a solution by introducing analytical chemical techniques to study lipids and lipidome [146, 147].

Lipidomics has emerged as a new field of omics technology, focusing on the comprehensive study of lipid species in a higher view to ultimately understand the detailed function of lipids in individuals. This approach has been pushed forward in different fields of health research, such as clinical diagnosis, where lipidomics has contributed to the discovery of several lipid biomarkers in the disease [148, 149]. For example, lipidomics has been conducted in studies of Alzheimer's disease (AD) [150], ischemia-reperfusion injuries Field [144] and cardiovascular diseases Field[151].

Lipidomics is primarily based on mass spectrometry (MS) analysis, with the incorporation of liquid chromatography (LC) to enable comprehensive analysis of lipid subclasses. Using different MS techniques, different branches of lipidomics

have been established for various purposes, such as targeted lipidomics analysis and multi-dimensional MS-based shotgun lipidomics.

Shotgun lipidomics is one of the most frequently used methods in lipidomics analysis due to its high-throughput analysing capability [135, 146]. This approach employs an orbitrap mass analyser, enabling the comprehensive characterisation and detection of the diverse physical and chemical properties of lipid molecules across different lipid classes, subclasses, and species. Additionally, LC is introduced in this analysis to further enhance the sensitivity of isomers. In conjunction with this LC-orbitrap MS system, a dedicated lipid analysing software, “Lipid Search”, has been developed to facilitate global lipid analysis [152, 153]. However, it is important to note that in the pursuit of high-throughput analysis, the sensitivity and specificity of shotgun lipidomics may be compromised, which makes it necessary to conduct further targeted lipidomics to achieve higher accuracy and precision [154].

Targeted lipidomics are involved in studies regarding specific lipid classes and species. Multiple reaction monitoring achieved with a triple-quadruple MS is widely used for targeted lipidomics analysis [155, 156]. The three quadruples allow monitoring of specific ionised molecules through the three times of fragmentation, which provide reliable accuracy to qualification and quantification in this targeted analysis. A representative example of the usage of targeted lipidomics is to detect those low abundance signalling lipid molecules such as sphingosine-1-phosphate, free fatty acids and fatty acid-derived metabolites [157-159]. Additionally, to analyse

metabolites that are unstable or difficult to be ionised, such as short-chain fatty acids (fatty acids with less than six carbons) [160], testosterone [160] and 4-hydroxyalkenal species [161], chemical derivatisation of samples will be required before analysis.

The metabolism of lipids is highly complicated as lipids can be modified among classes and subclasses through a massive metabolic pathway network [162]. The change of one single lipid spicy could typically relate to levels or activity of multiple enzymes and genes. After analysing lipid contents with lipidomics, it is crucial to link the alteration of lipids to the cell biology level. The ultimate strategy is to combine multiple omics together, undergoing statical analysis and testifying in vitro and vivo.

Chapter 2 Role of Intracellular Cholesterol Transporter ORP2 in Atherosclerosis-related Vascular Inflammation

2.1 Experiment Design

In this chapter, to address the role of intracellular cholesterol transporter ORP2 in atherosclerosis vascular inflammation, siRNAs and lentivirus-transduced shRNAs were used in vitro. After the knockdown of ORP2, inflammatory phenotypes of HUVECs were examined.

2.2 Methods and Materials

2.2.1 HUVEC Culture

Primary human umbilical vein endothelial cells (HUVECs, obtained from Prof. Jennifer Gamble, Centenary Institute, Australia) were cultured in polystyrene tissue culture flasks (Corning, #CLS-430639 #CLS-430641) that pre-coated with 2% gelatin (Sigma, #G9391) with HUVEC culture medium (Table 1). To pass HUVECs, remove the culture medium and rinse with PBS (Gibco, #14190250). Then, HUVECs were incubated with warm TrypLE (Gibco, #12604021) until 90% of cells were trypsinised. Wash cells with Medium 199 containing 2% of FBS, centrifuge at 200 g for 5 min and seed in new flasks. (0.3 million in T25 flasks or 1 million in T75 flasks). While seeding the cells, 15 μg/mL of heparin (Sigma, #H3393) and Falcon Endothelial Cell growth supplement (ECgs, Corning, #FAL356006) were added to the culture medium. After seeding, HUVECs were seeded in HUVEC medium and incubated at 37 ℃ and 5% CO_2.

Name	Volume	Manufacturer& category number
Medium 199	500mL	Sigma M4530-500mL
FCS (FBS)	100mL	Sigma F9423-500mL
HEPES (1M)	10mL	Thermo Fisher 15630-080
Sodium pyruvate (100mM)	5mL	Gibco 11360070
MEM non-essential amino acids	5mL	Gibco 11140050
Sodium bicarbonate (7.5%)	7.5mL	Gibco 25080-094
Penicillin/Streptomycin antibiotics	5mL	Gibco 15140122
Total	632.5mL	

Table 1. HUVEC medium ingredient

2.2.2 HEK293T Cell Culture

HEK293T was obtained from CellBank Australia. Cells were cultured in Dulbecco's modified Eagle medium (DMEM, Gibco, Cat#10569-010) with 10% fetal bovine serum (FBS, Hyclone) and 100 unit/mL Penicillin/Streptomycin antibiotics (Thermo Fisher, Cat#15140122).

2.2.3 THP-1 Cell Culture

THP-1 is human leukemia monocyte-like suspension cell line[163], and was obtained from Dr. Justin Wong's lab. THP-1 was cultured in RPMI 1640 medium (Gibco, #11875093) with 10% of FBS, 5 mL of 100X NEAA, 5 mL of 100X sodium pyruvate and 100 unit/mL of Penicillin/Streptomycin antibiotics. Cells were maintained within the density of $1.0x10^5$-$1.5x10^6$ cells/mL.

2.2.4 Lentivirus Packaging and Transduction

HEK293T cells were seeded in T25 flasks of 0.5 million per each. After overnight incubation in 37 ℃ and 5% CO_2, till the density of HEK293T reached 30%-50% of density, perform Lipofectamine LTX Reagent-based transfection (ThermoFisher, #15338100). The third generation of lentivirus vectors [164] was used in this research. pRSV-Rex (Addgene, #12253), pMDLg/pRRE (Addgene, #12251), pMD2.G (Addgene, #12259) and pLKO.1 (Sigma, # TRCN0000155678) were

transfected into HEK293T cells. 36-48 hours later, the culture medium was collected. Centrifuge at 300 g for 5 minutes, keep the supernatant and filter with 0.45 μm filter (Corning, #COR431225). Viruses can be used immediately or short-term stored at -80 ℃

The targeting sequence of shRNA is CAGAAAGTCACGGGAATGATT. Packaged lentivirus was loaded to infect HUVECs that were pre-seeded one day before and added 2 μg/mL of polybrene (Sigma, #H9268).

2.2.5 siRNA Transfection

HUVEC cells were seeded in T25 flasks of 0.3 million per each. Following overnight incubation at 37 ℃ and 5% CO2, the cells were allowed to reach a density of 30%-50%., perform Lipofectamine RNAiMAX-mediated transfection (ThermoFisher, #13778) to transfect control and ORP2 siRNA (GenePharma) to HUVECs at least 24 h prior to the stimulations.

2.2.6 Western Blotting

HUVECs are harvested after certain treatment with cell scraper in cold PBS and centrifuged at 300 g, 4 ℃ to remove PBS. Then cells were resuspended with approximately 30 to 100 μL of lysis buffer containing 50mM HEPES pH 7.4 (ThermoFisher, #15630080), 150 mM NaCl (Sigma, #S9888), 10% glycerol (Sigma, #G7893), 1mM of EGTA (Sigma, #E3889) and 1% of TRITON X-100 (Sigma,

#X100). Then sonicate the cells in lysis buffer in a Q800R2 sonicator (Qsonica) of 80% amplification for 10 min at 4 ℃. After sonication, samples were centrifuged at 1000 g, 4 ℃ for 5 min, then the supernatant was collected and transferred to a clean Eppendorf tube for BCA protein assay and gel loading.

For the BCA assay, BCA Protein Assay Kit (Sigma, #71285-M) was used for protein quantification. Following the manuscript offered by the company, samples were added to a 96-well plate along with BSA protein standards with the concentrations ranging from 0 to 20 mg/mL. After protein quantification, 20 μg of protein samples were mixed with 4X NUPAGE LDS Sample Buffer (ThermoFisher, #NP0007) and 10X NUPAGE Sample Reducing Agent (ThermoFisher, #NP0004) and then loaded into NuPAGE™ 4 to 12%, Bis-Tris, 1.0–1.5 mm, Mini Protein Gels (ThermoFisher, #NP0321) with 1x MOPS buffer (diluted from 20X MOPS buffter, ThermoFisher, #NP0001) in the gel tank. The protein electrophoresis was run at constant volt mode of 130 V for 60-90 min.

Following electrophoresis, proteins were transferred onto polyvinylidene fluoride (PVDF) membranes (Sigma, IPVH00010) using transfer buffer prepared by diluting 20X NUPAGE transfer buffer (ThermoFisher, #NP0005) at 320 mA for 90 min. Membranes were then blocked with 5% skim milk in PBS buffer containing 0.1% of Tween 20(PBST) for 1 h at room temperature. After blocking, the membranes were washed 3 times with PBST and incubated with primary antibodies overnight at 4 ℃. Following another three times of washes with PBST, the membranes were incubated with 1:1000 diluted anti-rabbit secondary antibody for 1 h at room temperature. Finally, the membranes were imaged using Bio-Rad ChemiDoc Touch, and the

signals were detected with ECL chemiluminescence reagent (ThermoFIsher, #WP20005).

To re-blot the membrane, bound primary and secondary antibodies were removed by incubating in stripping buffer (ThermoFisher, #46430) for 10-15 min at room temperature and then re-incubate with primary antibodies for further analysis.

Gel images were firstly processed with Image Lab 6.0.1 (Bio-Rad) and then quantify using ImageJ 1.53k.

Primary Antibody	Company	Catalogue number
rabbit anti-actin	Sigma	A2103
rabbit anti-cleaved caspase 1	Cell signaling technology	4199
rabbit anti-cleaved IL-1β	Cell signaling technology	83186
rabbit anti-IL-1β	Cell signaling technology	12703
rabbit anti-GAPDH	Cell signaling technology	97166
rabbit anti-OSBPL2	Proteintech	14751-1-AP
rabbit anti-NLRP3	Proteintech	19771-1-AP
rabbit anti-P-p65	Cell signaling technology	3033T
rabbit anti-p65	Cell signaling technology	3034
Rabbit anti-ICAM-1	Cell signaling technology	4915

Table 2. Antibodies used in western blotting.

2.2.7 E-selectin Immunofluorescence

Coverslips (Corning, #CLS285018) were decontaminated with 80% ethanol overnight, rinsed 3 times, and placed in a 6-well plate (Corning, #CLS3516). To coat the coverslip, 1.5 mL of 2% gelatine was added to each well and incubated at 37 ℃ for at least 15 minutes. $1x10^5$ of HUVECs are seeded into each well of the pre-coated 6-well plate with coverslips.

After 5 h of TNF-α treatment, cellular nucleuses were stained with NucBlue Live ReadyProbe Reagent (ThermoFisher, #R37605), then remove the culture medium, wash HUVECs with DPBS for 2 times and fix the cells with 4% formaldehyde (ThermoFisher, # 28908) for 15 minutes. After permeabilizing the cells with 0.2% triton X-100 (Sigma, #X100) in PBS for 15min at room temperature, block with 3% BSA at room temperature for 60 min. Primary anti-E-selectin antibody (Invitrogen, MA1-22165) was diluted 300 times to incubate with cells overnight at 4 ℃. The next day, rinse the slices with PBS twice and incubate them with the anti-mice secondary antibody (ThermoFisher, 488nm) for 1-2 hours at room temperature, avoiding light. Slices were mounted with ProLong Glass Antifade Mountant (ThermoFisher, #P36980), then moved to dark room while kept horizontally.

Immunofluorescence slices were imaged at the Facility of Sydney Microscopy & Microanalysis. Images were taken with a C2-confocal microscope (Nikon).

2.2.8 Monocyte Adhesion Assay

THP-1 cells were centrifuged and reconstituted to 1 million cells per mL in RPMI 1640 medium. To label live THP-1 cells with green fluorescence, 1 μL of 1 μg/mL Calcein-AM (ThermoFisher, #C1430) were added into each mL of cells and incubated at 37 ℃, avoiding light. After staining incubation, centrifuge cells at 200 g for 5 minutes and remove the medium. Cells were resuspended at 1 million cells/mL in the HUVEC culture medium. 1 mL of stained THP-1 cells were added to each pre-seeded monolayer of HUVECs that were treated or untreated with TNF-α in 6-well plates and incubated at 37 ℃ 5% CO_2 incubator for 1 hour. Remove the medium containing unattached THP-1 cells and gently wash HUVEC monolayers with RPMI 1640 medium for three times. Wash with PBS once and fix the cells with 4 % formaldehyde. Adherent THP-1 were imaged at 495/520 nm of excitation and emission wavelengths.

2.2.9 Statistical Analysis and Image Analysis

All statistical analyses were conducted with GraphPad Prism 9.0 software, and data were shown as mean ± standard deviation. Comparisons in this chapter were addressed with t-tests, and statistical significance was accepted at $p < 0.05$. Images were analysed with ImageJ (NIH) and Nikon Element (Nikon).

2.3 Results

2.3.1 Deficiency of ORP2 Reduces the Level of the Plasma Membrane (PM) Cholesterol.

Amphotericin B (AmB) is an antifungal agent that can bind to cholesterol on PM and form poles at binding sites to lead to cytoplasm leakage and cell death [3, 4] so that AmB treatment can be used to determine PM cholesterol level [5]. After AmB treatment, those cells with a higher level of PM cholesterol are more vulnerable to death. I found that AmB treatment induced HUVEC death in a dose-dependent manner (Fig. 2-1). Notably, ORP2 knockdown cells showed higher viability at 50 mg/L conc (90% vs. 60%) and 100 mg/L conc. (60% vs 20%), indicating decreased PM cholesterol levels.

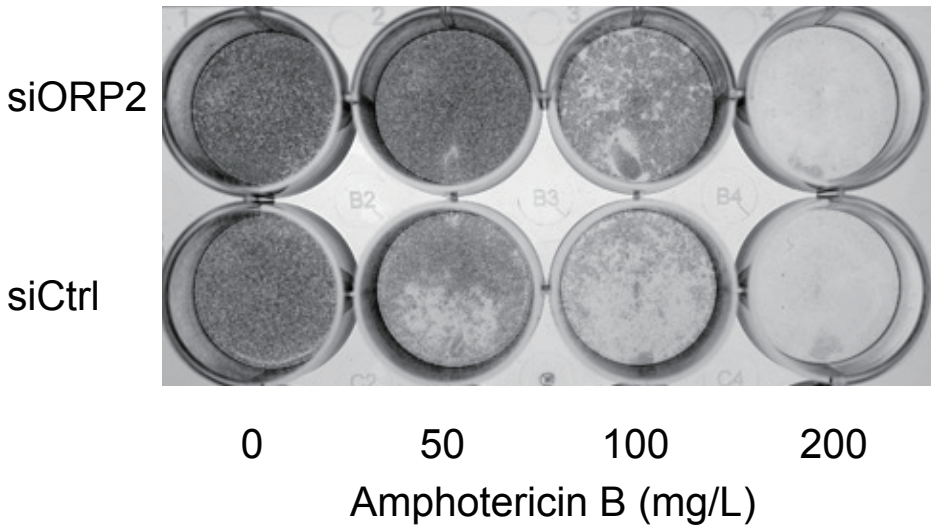

Figure 2-1. Knockdown of ORP2 reduces cell membrane cholesterol content.

ORP2 was knocked down by siRNAs in HUVECs. After AmphoB treatment (0, 50, 100, 200 mg/L), cells were stained with crystal violet and image in a bright field. By the concentration of 100 mg/L, 40% of siORP2 and 80% of siCtrl HUVECs were killed, which indicates that the knockdown of ORP2 reduces the PM cholesterol level of HUVECs.

2.3.2 ORP2 Deficiency Suppresses Inflammatory Signalling in HUVECs.

To define the role of ORP2 in vascular inflammation, I performed siRNA-mediated knockdown of ORP2 in HUVECs that were treated with 20 ng/μL TNF-α for five h and 24 h. A marked decrease in the levels of phosphorylated p65, the active form of nuclear factor NF-kappa-B (NFκB) and the established marker of pro-inflammatory signalling after the knockdown of ORP2 (Fig. 2-2). Meanwhile, total p65 levels were not changed (Fig. 2-2). Additionally, the expression levels of adhesion molecules ICAM1 and MCP-1 were decreased upon ORP2 deficiency (Fig. 2-2).

To simulate disturbed blood flow-mediated vascular inflammation *in vivo*, I exposed HUVECs to a disturbed flowing medium generated using an IBIDI pump. Knockdown of ORP2 reduced the expression of phosphorylated p65 and ICAM1 in HUVECs compared to control cells (Fig. 2-2). This, along with the TNF-a treatment, indicates an anti-inflammatory role of ORP2 deficiency in HUVECs.

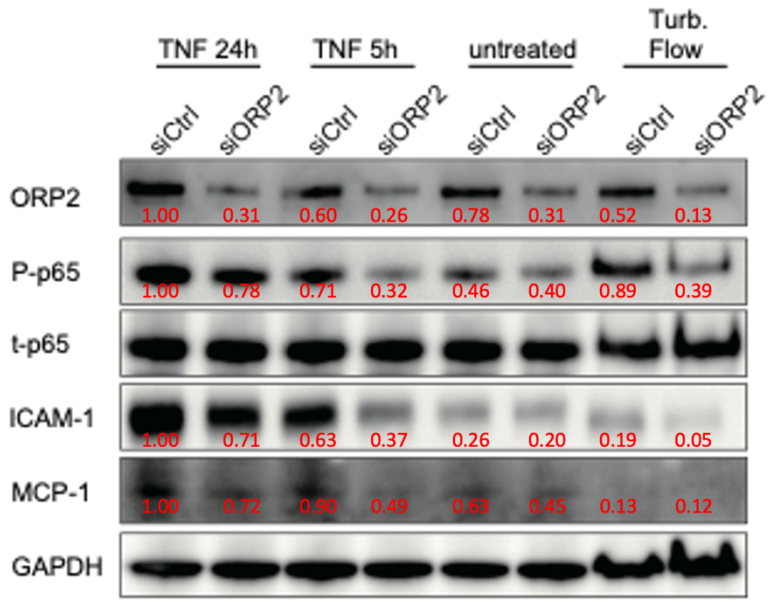

Figure 2-2. Knockdown of ORP2 with siRNA suppresses inflammatory signalling in HUVECs.

ORP2 was knocked down by siRNAs in human umbilical vein endothelial cells (HUVECs). Then, cells were treated with 20 ng/ml TNFα for the indicated times or exposed to turbulent (turb.) flow at 0.5±4 dyn/cm^2 for 24h. NFκB activation was determined by Western blotting of P-p65. The expression levels of adhesion molecules ICAM-1 and MCP-1 were also examined. P-p65 was quantified normalised to total p65, and ORP2, ICAM-1, MCP-1 were normalised to GAPDH. Each sample was pooled together from at least three different cords.

2.3.3 ORP2 Deficiency and Depletion of Cellular Cholesterol both Suppress Activation of TNF-α-Induced Inflammatory Signalling.

To consolidate these findings and investigate whether these were attributable to ORP2-mediated cholesterol regulation, I performed lentiviral shRNA-mediated knockdown in HUVECs and conducted comparative studies using a chemical-based cholesterol-depletion approach. Methyl-β-cyclodextrin (MβCD), a commonly used chemical, was utilised to deplete cellular cholesterol by binding with cholesterol and exporting cholesterol from the cell [165, 166]. I found that shRNA-mediated ORP2 knockdown also dramatically decreased phosphorylated p65 and ICAM1 levels in HUVECs (Fig. 2-3A). In addition, I pre-treated HUVECs with 1 μM MβCD 5 h prior to the addition of TNF-a. Notably, it was withdrawn when TNF-a was added. Pre-treatment with MβCD exhibited similar anti-inflammatory effects in cells exposed to TNF-a for 5 h (Fig. 2-3A, B). However, this chemical failed to suppress inflammatory responses when TNF-a treatment lasted for 24 h (Fig. 2-3A, B). This might be attributable to a recovery of cellular cholesterol levels after the removal of MβCD. Interestingly, MβCD pre-treatment also downregulated the levels of ORP2, while the changes in ORP2 levels were in line with pro-inflammatory signalling as seen in both 5 h and 24 h of TNF-a treatment.

Furthermore, I also examined the critical components of the inflammasome, including NLRP3, IL-1 and caspase-1. ORP2 knockdown and cholesterol depletion resulted in a decrease in NLRP3 expression (Fig. 2-3B). In addition, cleaved IL-1β and cleaved Caspase-1, both indicators of inflammasome activation, were downregulated with ORP2 knockdown and cholesterol depletion, along with pro-IL-

1β after 24 h of TNF-α stimulation. However, the expression of the other precursor pro-caspase-1 was found unaffected by TNF-α, ORP2 knockdown, or depletion of cholesterol.

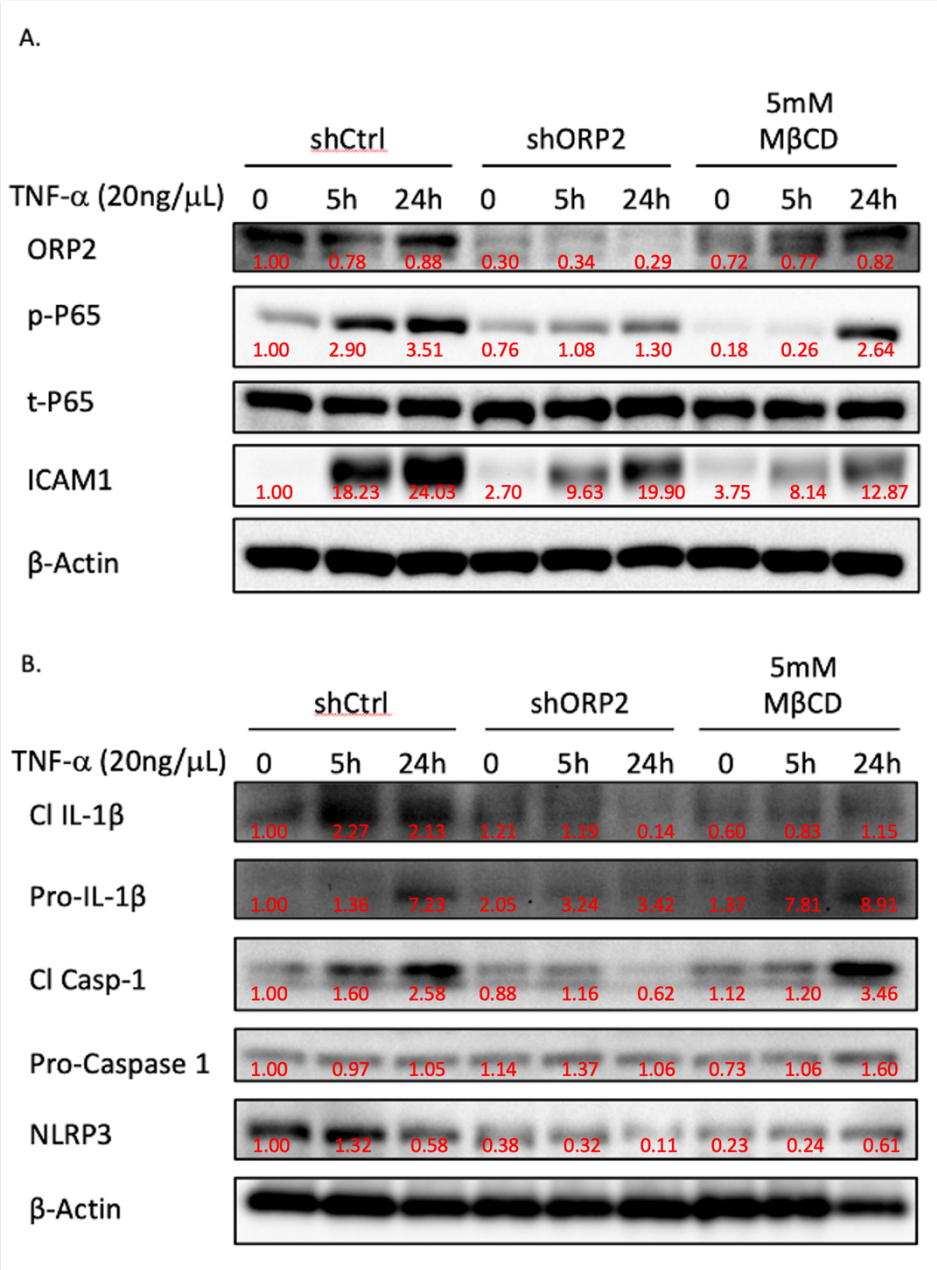

Figure 2-3. Knockdown of ORP2 with shRNA suppresses inflammatory signalling in HUVECs.

ORP2 was knocked down by shRNAs in human umbilical vein endothelial cells (HUVECs). Then, cells were treated with 20 ng/ml TNF-α for the indicated times. NFκB activation was determined by Western blotting of P-p65. The expression levels of adhesion molecules ICAM-1 were decreased after ORP2 KD (A). Inflammasome-related signalling was addressed by western blotting of NLRP3, and the cleaved form of IL-1β and Caspase-1 (B), and cl-IL-1β and cl-caspase1 were reduced after ORP2 Knockdown under the stimulation of TNF-α (B). P-p65 was quantified and

normalised to total p65, and the rest of the proteins were normalised to β-Actin. Samples were pooled together from at least three different cords.

2.3.4 ORP2 Deficiency Suppresses Expression E-selectin

To further address the anti-inflammation effect of ORP2 knockdown, I conducted immunofluorescence to visualise the expression of E-selectin induced by TNF-α. TNF-α treatment significantly increased E-selectin expression in HUVECs (Fig. 2-4A). In contrast, the knockdown of ORP2 decreased the expression levels of E-selectin by 71% (Fig. 2-4B). This data further demonstrates the anti-inflammatory effects of ORP2 deficiency.

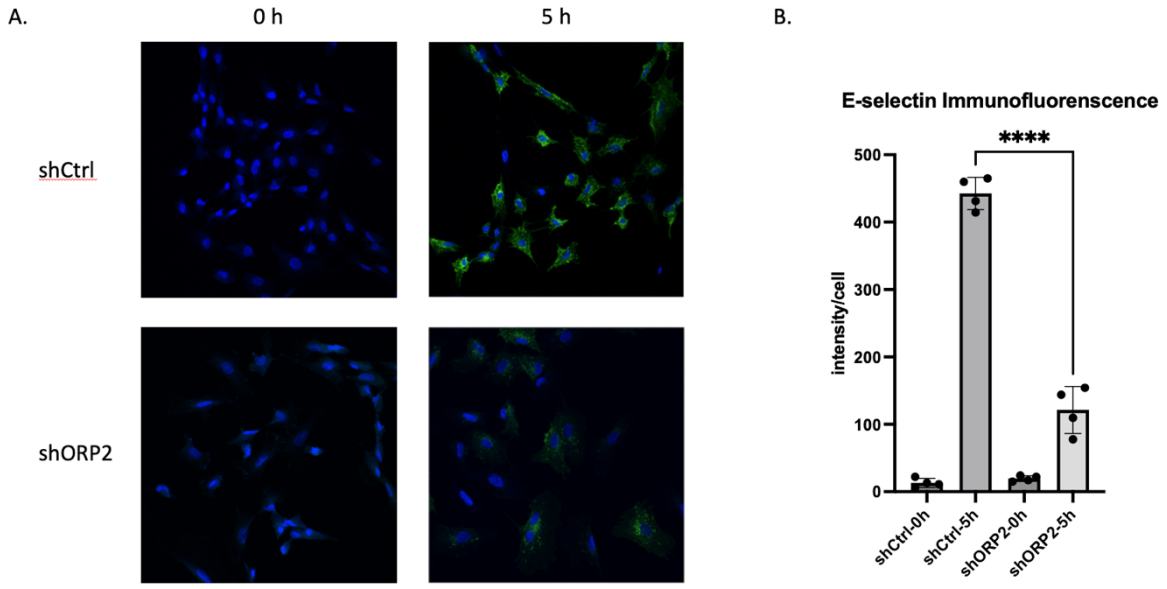

Figure 2-4. Knockdown of ORP2 suppresses the adhesion molecule E-selectin.

ORP2 was knocked down by shRNAs in human umbilical vein endothelial cells (HUVECs). Then, cells were treated with 10 ng/ml TNFα for 5 h. Expression of E-selectin was determined with immunofluorescence (A) and was quantified (B). The expression of E-selectin activated by TNF-α was significantly decreased after ORP2 knockdown. Statistics were performed by unpaired t-test with Prism 9, ****p<0.0001.

2.3.5 ORP2 Deficiency Mitigates Monocyte Recruitment to HUVEC Monolayer

One of the major pathological consequences of vascular inflammation is increased recruitment of monocytes to endothelium, which is followed by immune cell infiltration and elevated local tissue inflammation, as seen in multiple chronic diseases. Therefore, I measured monocyte adhesion to HUVEC monolayer in response to TNF-α-stimulation. To this end, I first labelled THP-1 monocytes using Calcium AM. Subsequently, I incubated fluorescently labelled monocytes with both shORP2 and shCtrl HUVECs. In the absence of TNF-α-stimulation, monocyte recruitment to the HUVEC monolayer was minimal (Fig. 2-5A). In contrast, with the 5 h TNF-α treatment, pronounced monocyte recruitment was induced in control cells (Fig. 2-5A), while it was significantly decreased by 79% in ORP2 knockdown HUVECs (Fig. 2-5B).

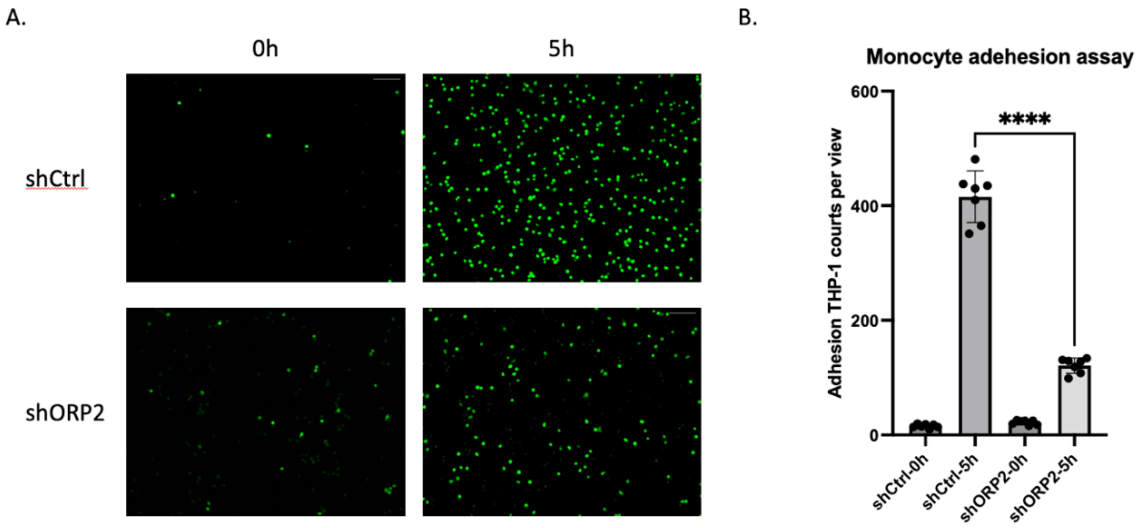

Figure 2-5. Knockdown of ORP2 inhibits monocyte adhesion in HUVECs.

Monocyte adhesion assay was performed with ORP2-knockdown HUVECs after treatment with TNF-α for 0 and 5 h (A) and quantified (B). Recruitment of THP-1 under treatment of TNF-α was significantly reduced after ORP2 knockdown. Statistics were performed by unpaired t-test with Prism 9, ****p<0.0001.

2.3.6 ORP2 Deficiency and Lipid Rafts

Cholesterol is instrumental for lipid raft formation within the PM. It is intriguing to investigate whether ORP2 deficiency altered the expression of raft proteins. However, neither Flot-1 nor Cav-1, two crucial structural proteins associated with lipid rafts, exhibited notable changes in response to TNF-α stimulation or ORP2 knockdown.

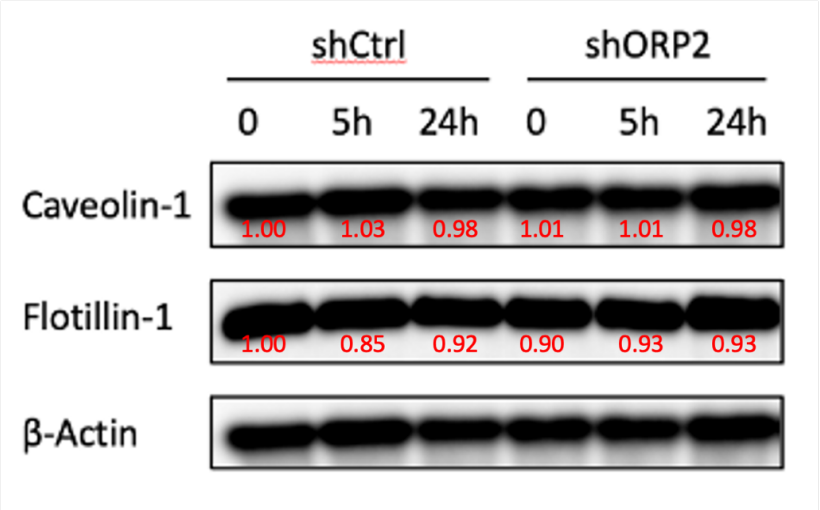

Figure 2-6. Knockdown of ORP2 did not interrupt the expression of lipid rafts-related proteins in HUVECs.

Lipid raft structural proteins, Flotillin-1 and Caveolin-1, were analysed with western blotting. The levels of Flot-1 and Cav-1 were not changed after ORP2 knockdown. *Cav-1 and Flot-1 were normalised to β-Actin. Samples were pooled together from at least three different cords.*

2.4 Discussion

In this chapter, I demonstrated ORP2 knockdown in Human umbilical vein endothelial cells (HUVEC) and tested the anti-inflammation effect of ORP2 knockdown. The major finding of this chapter shows that ORP2 knockdown suppresses endothelial activation and following inflammation signalling activation under stimulation of TNF-α and turbulent flows by attenuating the activation of NFκB (Fig. 2-2, Fig. 2-3), adhesion molecules (Fig. 2-3, Fig. 2-5) and NLRP-3 inflammasome signalling (Fig. 2-4). THP-1 adhesion in response to TNF-α is also reduced by ORP2 knockdown in HUVECs (Fig. 2-5). The anti-inflammation effect is not approached by disturbing the expression of lipid rafts structural proteins (Fig. 2-6).

In previous studies, knockdown or knockout of ORP2 has been proven to reduce the accumulation of PM cholesterol in HeLa cells [121, 122] and HUVECs [129]. In a previous study, deficiency of ORP2 was shown to inhibit angiogenesis by blocking VEGFR2 signalling in both vitro and vivo [129]. The function of ORP2 is to transport newly synthesised cholesterol from ER to the PM, which has been earlier proven at overexpression cellular level [167] and protein structural level [121].

Amphotericin B resistance experiment shows a lower level of PM cholesterol in ORP2 knockdown HUVECs, compared to it in siCtrl. However, PM cholesterol in the ORP2 shRNA-knockdown HUVEC was earlier reported to be without a significant reduction by Koponen et al [129]. Considering that different methods of knockdown (siRNA & shRNA) and different detection strategies (Amphotericin B & D4H-fluorescent probes) were used in two different research studies, this contradiction is not surprising.

More importantly, The D4H probe used in that research is expressed within the cell and more likely to bind and detect cholesterol in the inner cytoplasmic side of PM, while the amphotericin B resistance acts with the cholesterol on the outside of PM. Moreover, both techniques are indirect ways to detect cellular cholesterol. To solve this issue, I am planning to perform PM isolation and analyse PM cholesterol with targeted lipidomics to further testify in the future.

The reduction of phosphorylation of p65 indicates that the activation of transcriptional factor NFκB under stimulation of both TNF-α and turbulent flows was inhibited in ORP2 knockdown HUVECs. The formation of NLRP3 inflammasome is also disrupted in ORP2 knockdown HUVECs with the reduction of NLRP3 and cleavage forms of IL-1β and caspase-1. Interestingly, pro-IL-1β is also found to be reduced under ORP2 knockdown and cholesterol depletion with MβCD. The transcription of IL-1β relies on the regulation of NFκB, which is activated by TNF with the action of TNF receptor 1(TNFR1) [168], which associates with PM microdomain lipid rafts [100].

Additionally, in this study, the knockdown of ORP2 can also inhibit the expression of adhesion molecules in HUVECs and the subsequent monocyte adhesion. The recruitment of immune cells that happens during endothelial activation is approached by the collective effects of multiple adhesion molecules. In endothelial cells, the expression of these adhesion molecules, including ICAM-1 [31, 169] and E-selectin [32, 170], are all induced by NFκB in response to TNF-α or IL-1β. The recruitment of THP-1 cells after the knockdown of ORP2 in HUVECs is also shown to be reduced.

The response of TNFR1 after activated by TNF-α requires the recruitment of TNFR1-associated death domain protein (TRADD) [171] to initiate downstream signalling

and ultimately leads to the activation of NFκB [172]. After the trigger of TNF-α TNFR1 and its coupled signalling molecules were found to translocate to lipid rafts. This translocation has been reported in HT1080 cells [100], HeLa cells [173] and fibroblasts [174]. Depletion of cholesterol in HT1080 cells with MβCD has been reported to inhibit the translocation of TNFR1 and, therefore, disrupt the activation of NFκB [100], which is consistent with my result of MβCD treatment in HUVECs.

PM is not made of an even distribution of lipids. Instead, there are lipid microdomains called lipid rafts existing in PM [99, 175]. Lipid rafts are enriched with free cholesterol and sphingolipids, including sphingomyelin and glycosphingolipids. Lipid rafts can conduct signalling pathways as numerous receptors are docked at this microdomain.

Deficiency of lipid rafts structural protein caveolin-1 (Cav-1) was reported to attenuate vascular inflammation and atherosclerosis [176-178]. Deficiency of Cav-1 in endothelium can enhance eNOS-derived NO synthesis [177] and low-density lipoprotein [178]. And overexpression of Cav-1 in endothelium can accelerate atherosclerosis [179].

The anti-inflammatory effect of ORP2 knockdown seems to point to disrupting lipid rafts. However, the expression of two of the major structural proteins, Flot-1 and Cav-1, were not altered after the knockdown of ORP2. The limitation of this study is I could not successfully directly examine the integrity of lipid rafts yet. Compared to the depletion of cholesterol with MβCD, the ORP knockdown that I conducted is a mild way to reduce PM cholesterol level, which might not completely block the formation of lipid rafts but inhibits the function and biophysical properties of lipid

rafts. To further testify to the function of ORP2 knockdown in regulating lipid rafts, It is worth starting with examining the integrity of lipid rafts.

Apart from the stimuli of TNF, the anti-inflammatory effect of ORP2 deficiency also works in the OSS stimulation. The aligned shear stress, recognized for its protective impact on blood vessels, has been documented as having the ability to decrease PM (plasma membrane) cholesterol levels. Consequently, this reduction could enhance mitochondrial function, leading to increased ATP biosynthesis and decreased release of reactive oxygen species (ROS) [180]. My hypothesis regarding the effect observed in Fig. 2-2 is that the decrease in PM cholesterol resulting from ORP2 knockdown has the potential to counteract the pro-inflammatory effect induced by OSS. However, further validation is necessary to substantiate this claim.

In conclusion, the knockdown of ORP2 has been shown to effectively inhibit the proinflammatory action of endothelial activation by reducing plasma membrane cholesterol levels. This suggests that ORP2 and PM cholesterol could be potential targets in studies of cardiovascular diseases. Meanwhile, membrane biological study of the knockdown of ORP2 is required to testify to the mechanism of this anti-inflammation effect of ORP2 knockdown.

For future works, I have successfully generated an ORP2 endothelial-specific knockout (ORP2-EKO) along with an ApoE global knockout mouse model. The endothelial-specific knockout is achieved by crossbreeding floxed ORP2 mice with cdh5-cre mice [181]. The animal experiment will start with inducing atherogenesis in ApoE/ORP2-EKO double-knockout mice by feeding a high-fat, high-cholesterol diet, followed by studies on physiological, pathological, and biochemical levels of atherosclerosis in mice. Besides, lipidomics analysis of PM cholesterol and integrity

of lipid rafts will be examined after membrane isolation of ORP2 knockdown HUVECs.

Chapter 3 Lipid Profiling of Senescent Endothelial Cells

3.1 Experiment Design

To scan lipid profiles in senescent endothelial cells, H_2O_2-induced senescent HUVECs were used in this chapter. HPLC/MS-based lipidomes were used to read the lipid contents of HUVECs during the initiation and late time of senescent HUVECs.

3.2 Material and Methods

3.2.1 Endothelial Senescence Inducement

HUVECs were seeded at 0.3 million cells/T25 in HUVEC culture medium overnight till reaching the density of approximately 30%. Then, cells were treated with 300 μM of H_2O_2. 24 hours later, remove the medium containing H_2O_2 and cells are kept in HUVEC medium at 37 ℃ 5% CO_2 incubator till Day 3 and Day 7 to run further assays. Fresh HUVEC culture medium will be changed every three days.

3.2.2 Senescence-associated β-Galactosidase (SA-β-Gal) Staining

SA-β-Gal was performed with a commercial kit (Cell Signaling, #9860), and the staining procedure was followed with the company's standard protocol.

At designated time points, remove the growth medium from the cells and wash with PBS twice. Then, fix cells with dilutant from the 10x fixative solution in the kit for 10-15 min at room temperature. After another two times of PBS rinsing, add 1 mL of pH 6.0 β-Galactosidase staining solution to each 35 mm well of HUVECs. For each

testing 35 mm well of HUVECs, the staining solution is made up of 930 µL 1X Staining Solution, 10 µL 100X Solution A, 10 µL 100X Solution B and 50 µL 20mg/mL X-gal stock solution (in dimethylformamide), whose pH has to be adjusted within 5.9-6.1 strictly. HUVECs with the staining solution were incubated at 37 °C, CO_2-free and dry incubator for at least overnight. Cells were then imaged with a Nikon NiE microscope in a bright field.

3.2.3 Lipid Extraction

HUVECs at Day 0, Day 3, and Day 7 after H_2O_2 treatment were harvested in PBS, centrifuged at 300 g for 5 min, and resuspended in 1 mL of methanol (Sigma, #34860). Add 50 uL of internal standard and 4 mL of Methyl tert-butyl Ether (MTBE, Sigma, #34875) and sonicate samples at 4 °C for 30-60 min. After the sonication, add 1 mL of Optima water (Sigma, #270733), vortex for 30 s and centrifuge at 4,000 g for 10 min till the aqua phase and organic phase separate nicely. Collect the organic phase in the upper level to a new clean glass tube and speedvac organic phase till completely dry. Reconstitute lipids with 400 µL of 80% methanol in water, centrifuge at maximum speed to remove any insoluble precipitation and transfer to HPLC autosampler vials (ThermoFisher, #CHSV9-10P) and ready to run.

3.2.4Lipidomic Analysis Internal Standard Preparation

As there is an uncertainty of sensitivity for a long-time running mass spectrometer, it is necessary to introduce internal standards into analysing samples to give promising

results. A master mix of internal standards was prepared before lipid extraction with the following contents in Table 2.

Compound	CatLog	Company	Final amount in each sample/nmol
C17 Ceramide (Cer) (d18:1/17:0)	860517	Avantilipids	2.000
17:0 sphingomyelin (SM) (d18:1/17:0)	860585	Avantilipids	2.000
C17 Glucosyl(ß) Ceramide (d18:1/17:0)	860569	Avantilipids	2.000
Sphingosine (Sph) (d17:1)	860640	Avantilipids	0.200
Sphingosine-1-Phosphate (S1P) (d17:1)	860641	Avantilipids	0.200
Phosphatidylcholine (PC) (19:0/19:0)	850367	Avantilipids	5.000
Lyso-PC (17:0)	855676	Avantilipids	2.000
Phosphatidylserine (PS) (17:0/17:0)	840028	Avantilipids	2.000
Lyso-PS (17:1)	858141	Avantilipids	2.000
Phosphatidylethanolamine (PE) (17:0/17:0)	830756	Avantilipids	2.000
Lyso-PE (17:1)	856707	Avantilipids	2.000
Phosphatidic acid (PA) (17:0/17:0)	830856	Avantilipids	2.000
Lyso-PA (17:1)	857127	Avantilipids	0.020
Lyso-PI (17:1)	850103	Avantilipids	0.040
Lyso-PG (17:1)	858127	Avantilipids	2.000
d7-Phosphatidylinositols (PI) (15:0/18:1)	791641	Avantilipids	2.000
Phosphatidylglycerols (PG) (17:0/17:0)	830456	Avantilipids	2.000
Cardiolipin (CL) (14:0/14:0/14:0/14:0)	750332	Avantilipids	2.000
Triacylglycerol (TAG) (17:0/17:0/17:0)	16489	Cayman	2.000
D7-diacylglycerides (DG) (15:0/18:1)	791647	Avantilipids	2.000
Cholesteryl ester (ChE) (17:0)	700186	Avantilipids	2.000
D7-cholesterol (Chol)	25265	Avantilipids	2.500
Oleic acid -d9	861809	Avantilipids	5.000

Table 2. Information on internal standards.

3.2.5 Quantitative Reverse Transcription Polymerase Chain Reaction (RT-qPCR)

To measure mRNA levels in HUVECs, an RT-qPCR assay was performed. Total RNA was extracted from HUVECs using the TRIzol reagent (ThermoFisher, #15596026). According to the manufacturer's instructions, HUVECs were lysed by adding 300 μL of TRIzol into each T25 flask of HUVECs and pipetting the lysate several times to homogenise. After 5 min of incubation, add 0.2 mL of chloroform per 1 mL of TRIzol lysate and incubate for 2-3 min. Then centrifuge the sample at 12000 g at 4 °C for 15 min and transfer the aqueous phase containing RNA to a new tube. After that, add 0.5 mL of isopropanol per each 1 mL of TRIzol used for lysis to the aqueous phase from the last step and incubate for 10 min at 4 °C. Following incubation, samples were centrifuged for 10 min at 10000 g at 4 °C. Discard the supernatant, resuspend the pellet in 75% ethanol and centrifuge for 5 min at 4 °C and discard the supernatant to wash the RNA samples. Resuspend the washed RNA samples with RNase-free water containing 0.1 mM EDTA. Then the samples were incubated in a heat block at 60 °C for 10-15 min.

RNA concentration was tested with a NanoDrop spectrophotometer (ThermoFisher), and cDNA was synthesized from 1 μg of total RNA using the SuperScript III First-Strand Synthesis System (ThermoFisher, #18080051) with random primers. The reverse transcription reaction was performed at 25 °C for 5 minutes, followed by 50 °C for 60 minutes, and then terminated by heating at 70 °C for 15 minutes.

The RT-qPCR reaction was conducted in LightCycler 480 system (Roche), and the ORP2 mRNA expression levels were calculated using the 2^-ΔΔCt method with GAPDH as the internal control. The primer sequence of ORP2 was:

and the mean values were used for analysis. Statistical analysis was carried out using a paired t-test, and $p < 0.05$ was considered statistically significant.

The sequences of primers are as below. Forward: TCTGGGGAATTTTCAGAGGCA, reverse: GGCAGCGATGTCCTGTGTTT

3.3 Results

3.3.1 Lipid Profile is Altered in Senescent HUVECs

To understand the roles of lipids in endothelial cell senescence, I employed both global and targeted lipidomics to assess the alterations in lipid profiles of non-senescent, early senescent and late senescent HUVECs at day 0, 3 and 7 post-pretreatments with 300 mM H_2O_2 for 24 h, respectively (Fig. 3-1A). Herein, early senescence refers to the stage where cells have undergone genetic and metabolic reprogramming and have been engaged in the process of cellular senescence. In contrast, late senescence refers to the stage where cells have gone through significant morphological changes and exhibit elevated senescence-associated secretory phenotype (SASP). In this stage, cells have lost their proliferative capacity entirely, but paradoxically, they exhibit increased metabolic activity.

By the submission of this thesis, I have quantified 336 lipid species across 5 major lipid categories, namely FFAs, sphingolipids, phospholipids, glycerolipds and sterol lipids (Fig 3.2B). These were further sub-divided into 25 lipid classes, including phosphatidylcholines (PCs), phosphatidic acids (PAs), phosphatidylethanolamines (PEs), phosphatidylserines (PSs), Ceramides (Cers) were negligible. However, during the onset of senescence, it exhibited an upregulation in phosphatidylglycerols (PGs), phosphatidylinositol (PIs), cardiolipins (CLs), Phosphatidylethanolamine plasmalogens (PEps), lysophosphatidylethanolamines (LPEs), bis-methyl phosphatidic acids (BisMePAs), saturated fatty acids (SFAs), monounsaturated fatty acids (MUFAs), polyunsaturated fatty acids (PUFAs), hexosylceramides (HexCers), sphingomyelins (SMs), sphingosines (Sphs) and cholesterol (Chol).

Remarkably, there was a decrease in lysophosphatidylcholine (LPCs) and sphingosine 1-phosphates (S1P) (Fig. 3-1C).

The majority of lipid classes exhibited a significant increase along with the progression of senescence in HUVECs, with total PG, total PUFA and total HexCer showing the most dramatic increases of 129%, 200% and 213% on Day 7, respectively (Fig. 3-1C). Interestingly, total LPC and total S1P were profoundly decreased in this process by 40% and 50% on Day 7, respectively (Fig. 3-1C). This phenotype was also shown in the volcano plots displayed in individual species, where PGs, PUFAs and HexCer were increased while LPCs and S1P were decreased (Fig. 3-1D).

A.

B.

		Number of detected species
Phospholipid	PC	30
	PA	5
	PE	26
	PG	14
	PI	19
	PS	23
	CL	20
	Pep	25
	BisMePA	9
	LPC	24
	LPE	18
	LPI	2
	LPG	1
	LPS	1
Free fatty acid	SFA	6
	MUFA	4
	PUFA	5
Sphingolipid	Cer	26
	HexCer	17
	SM	27
	Sph	3
	S1P	2
Sterols	Cholesterol	1
Glycerolipids	DAG	29
	Total	336

C.

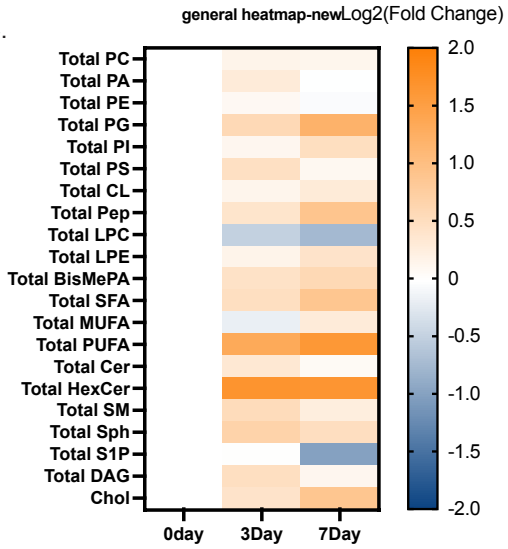

D.

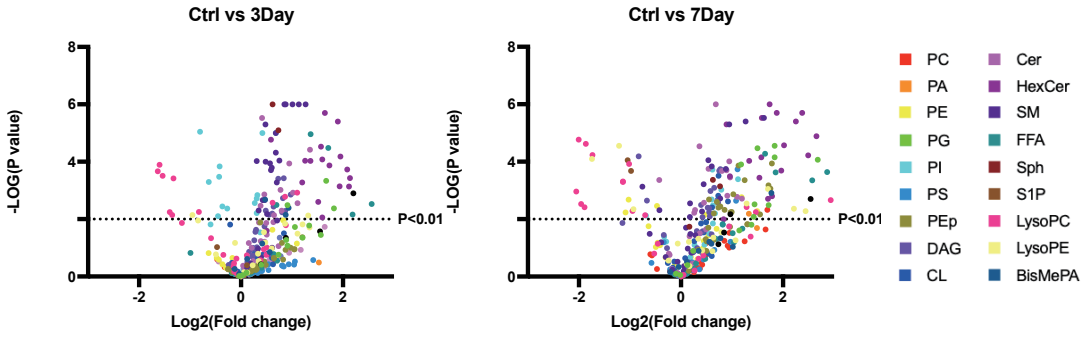

Figure 3-1. General summary of lipid profiling in senescent HUVECs.

HUVECs were treated with H2O2 and harvested following the experimental timeline (A). 336 of lipid species were detected and analysed by submission (B). Heatmap analysis (C) were generated to visualize the overall changes in lipid composition during the progression of senescence. Most of the lipid classes were observed to be upregulated in senescence, especially PG, PUFA and HexCer, however, total LPC and S1P were observed in decreases (C). Volcano plots were generated to show changes of individual species (Left: Ctrl vs. Day 3, right: Ctrl vs Day 7), x axis represents log2 of fold change (senescence to control) and y axis represents -log10 of p values from unpaired t-test performed with Prism 9 (D).

3.3.2 Increased Conversion of Ceramide to Complex Sphingolipids in Endothelial Cell Senescence

In the following work, I analysed the changes in individual lipid species during the progression of endothelial cell senescence. The well-known lipotoxic ceramide species d18:1/16:0 was significantly increased by 20% in late senescent ECs (Fig. 3-2A). In line, d18:1/16:0 sphingomyelin levels were increased by 23% and 13% in early and late senescent HUVECs, respectively (Fig. 3-2A). Interestingly, d18:1/16:0 hexceramide exhibited a much more dramatic increase (235% In early and 198% in late) as compared to sphingomyelin (Fig. 3-2B). Meanwhile, the levels of other major hexCeramide species were also elevated (Fig. 3-2B). Sphingomyelins and hexCeramides are the most abundant sphingolipids in cells, which are reversibly converted from ceramides. My results indicate an altered sphingolipid metabolic flux in EC senescence.

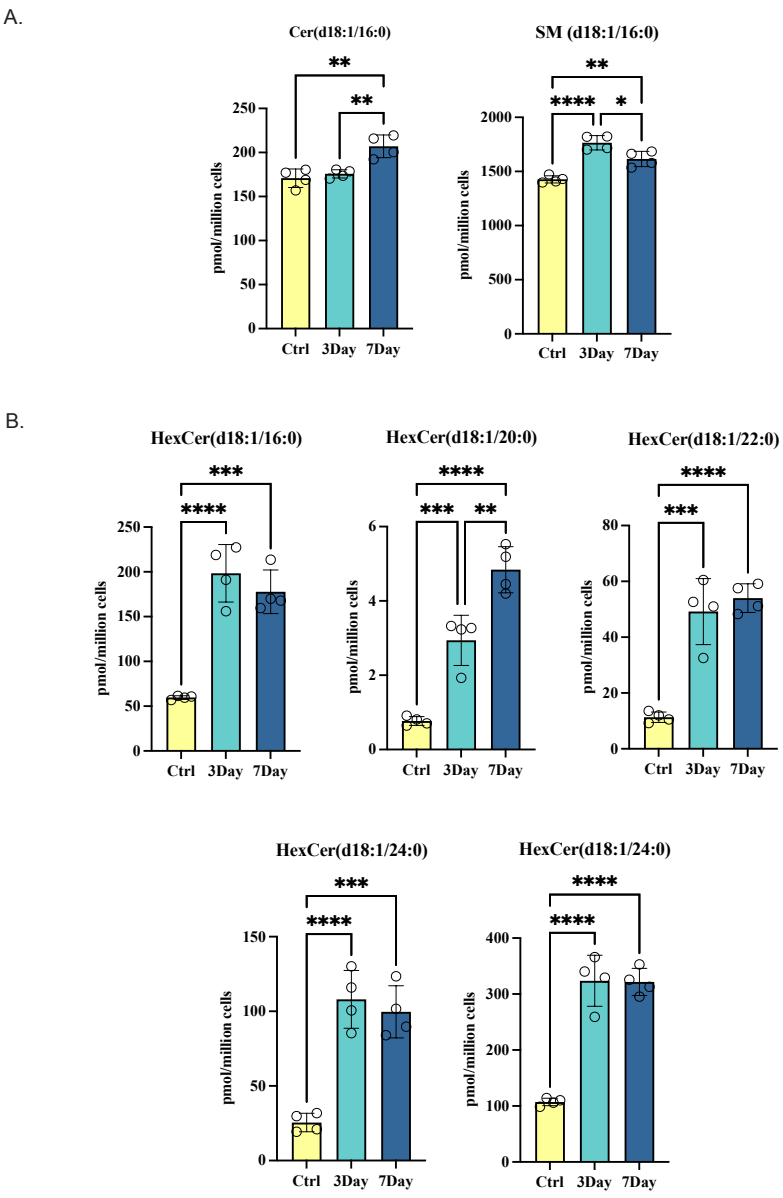

Figure 3-3. Levels of sphingolipids was changed in senescent HUVECs.

*Representative species of ceramide (left) and sphingomyelin (right) exhibited a mild increased in senescent HUVECs (A). Hexceramides were found decreased notably in senescence (B). Statistics were performed by ordinary one-way ANOVA with Prism 9, *p<0.05, **p<0.01, ***p<0.001, ****p<0.0001.*

3.3.3 Alteration of Glycerophospholipid in EC Senescence

As aforementioned, total PG levels were increased in EC senescence. Specifically, I found that PG (16:0/18:1), (16:0/20:4), (18:0/20:4) and (22:6/22:6) contributed most to this change (Fig. 3-3A).

In contrast, although the overall content of PIs exhibited an upregulation of 41% on Day 7 (Fig. 3-3B), the individual PI species were altered differentially. In general, those PIs containing saturated fatty acyl chains and monounsaturated fatty acyl chains, such as (d16:1/18:1), (d18:0/18:1) and (d18:1/18:1), were significantly decreased, whereas those bearing polyunsaturated fatty acyl chains, such as (d16:0/20:4), (d18:0/20:4), (d18:0/20:5), (d18:0/22:4) and (d18:0/22:5), were profoundly increased. Particularly, the most substantial increase was observed in PI (18:0/20:5) of 73% on Day 7 (Fig. 3-3B). Similarly, cardiolipin (CL) species with high degree fatty acyl chain unsaturation, including (72:9) and (74:9), were significantly upregulated by 65% on Day 7 (Fig 3-4C).

Distinct from the unchanged total PE levels, PE-plasmalogen (PEp) exhibited a significant increase. Those abundant PEp species, such as PE (16:0p/22:4), (18:0p/20:4) and (16:1p/22:5), exhibited notable upregulations by 228%, 237% and 193%, respectively (Fig. 3-4D).

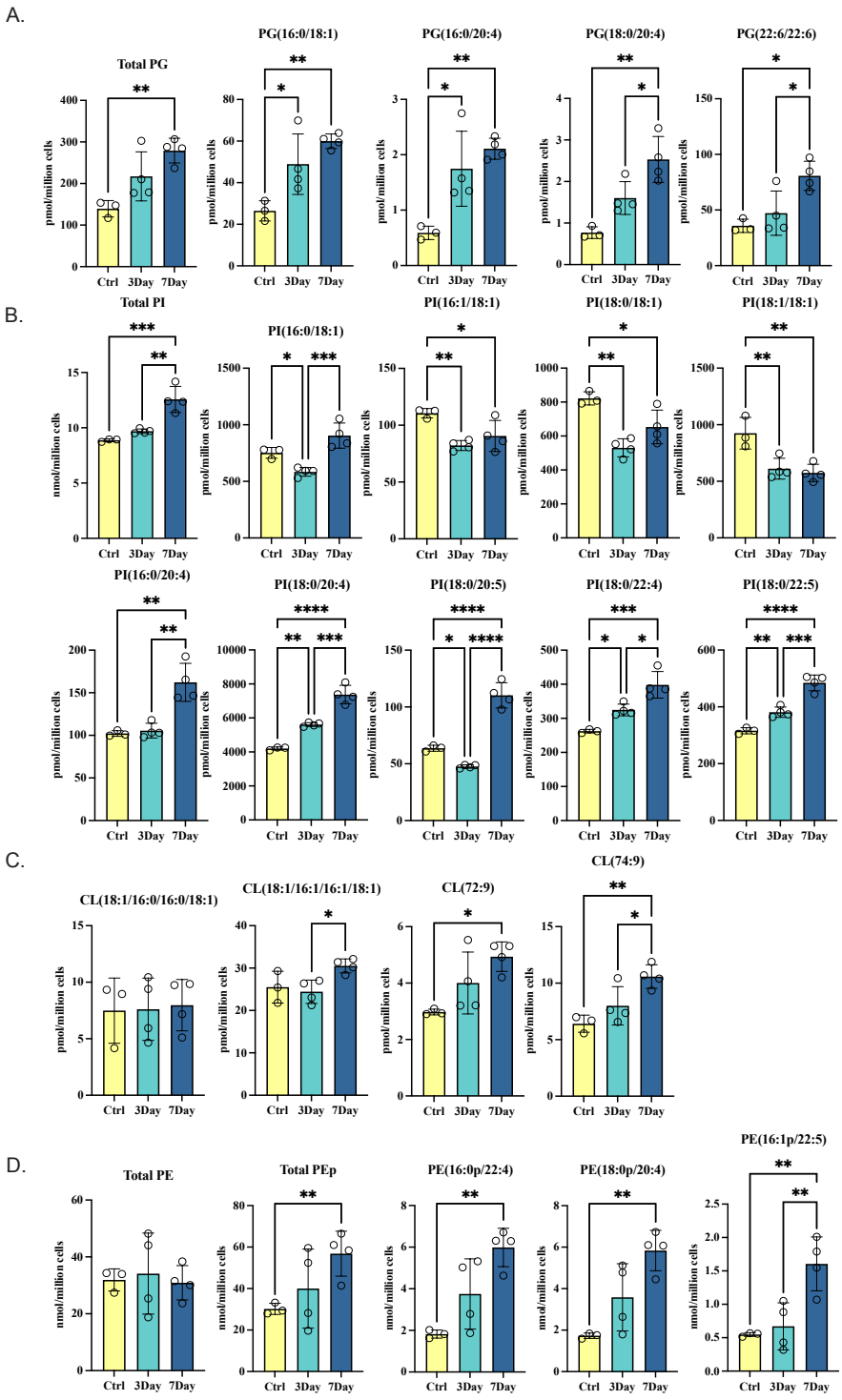

Figure 3-3. Fatty acyl-dependent alterations were found in glycerophospholipids.

Total and representative Phosphatidylglycerols (A), phosphatidylinositols (B) and cardiolipins (C) were shown. PGs exhibited a consistent increase during the progress of senescence (A). PI and CL demonstrated fatty acyl-dependent

*alterations: SFA/MUFA-only species exhibited decrease or no change while PUFA-containing species exhibited significant increase. Plasmalogen phosphatidylethanolamines (D) were observed to be upregulated. Statistics were performed by ordinary one-way ANOVA with Prism 9, *p<0.05, **p<0.01, ***p<0.001, ****p<0.0001.*

3.3.4 Notable Changes in Lysophospholipids in EC Senescence

I found that the levels of total LPC were downregulated by 29% on Day 3 and 41% on Day 7, with major contributors as LPC (16:0), (16:1) and (18:1) (Fig. 3-4A). In contrast to LPC, levels of total LPE were found decreased while there is not a significance (Fig. 3-4B). Interestingly, LPCe (ether-linked LPC) and LPEe were increased by 45% and 83% on day 7, respectively (Fig. 3-4C).

Furthermore, LPS (18:0), LPI (18:0) and LPG (22:6) exhibited significant increases in senescent ECs (Fig. 3-4D). Especially, a marked upregulation of 664% was observed in the level of LPG (22:6) on Day 7 (Fig. 3-4D).

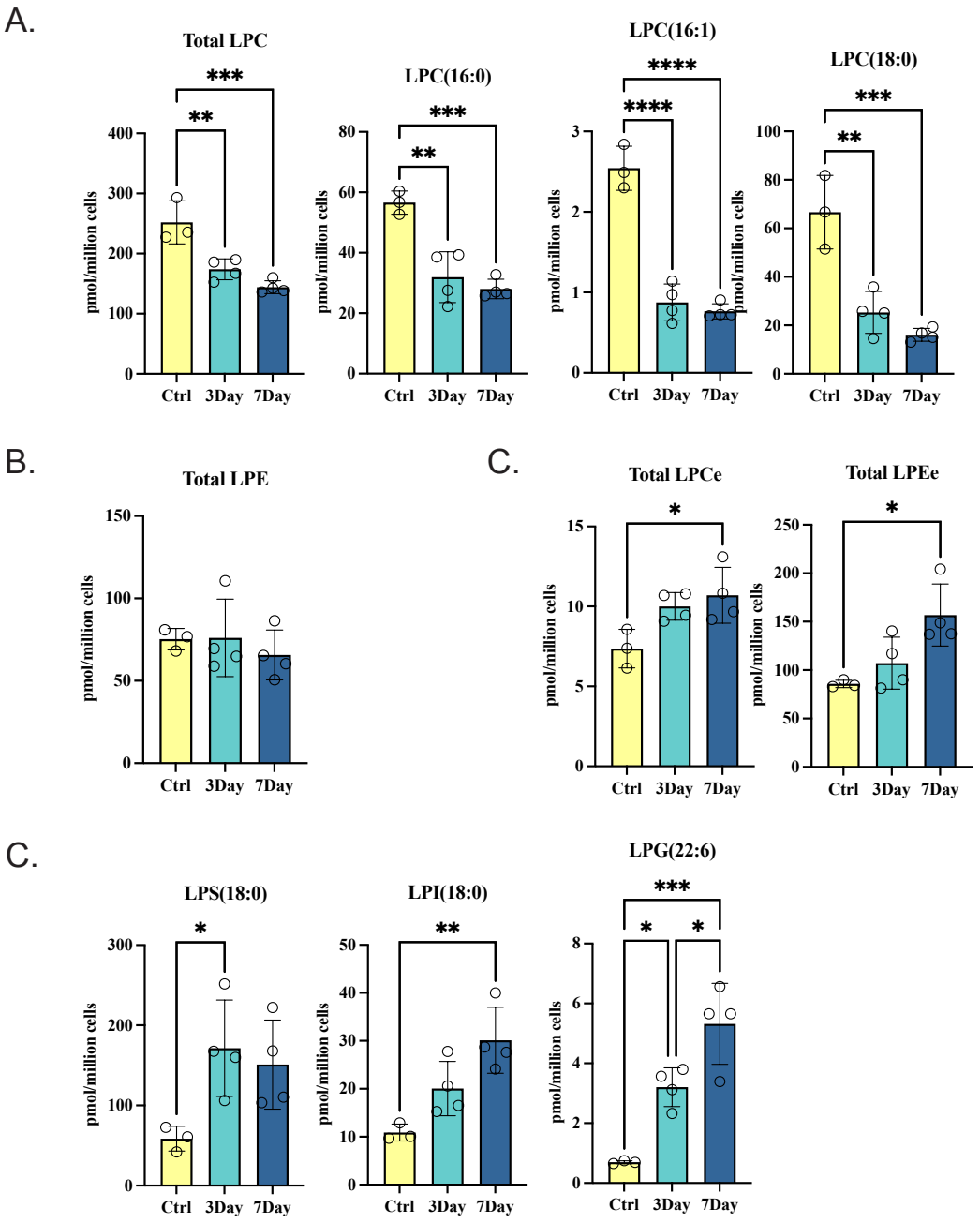

Figure 3-4. Changes of lysophospholipids in EC senescence.

*LPC (A) and LPE (B) were obereved to be downregulated while LPCe and LPEe were increased (C). Meanwhile, other lysophospholipids exhibited upregulation in EC senescence. Statistics were performed by ordinary one-way ANOVA with Prism 9, *p<0.05, **p<0.01, ***p<0.001, ****p<0.0001.*

v

3.3.5 Polyunsaturated Free Fatty Acid Levels Increased in EC Senescence.

We have developed “in-house” methods for a targeted quantitation of free fatty acids in senescent HUVECs. The total content of saturated free fatty acids (SFA) exhibited an upregulation; however, no significant changes were identified due to the variation (Fig. 3-5A). The overall quantity of monounsaturated free fatty acids (MUFA) remained unalteredin senescent HUVECs compared to non-senescent controls (Fig. 3-5A).

The marked changes were observed in the levels of total polyunsaturated free fatty acids (PUFAs), which was significantly upregulated by 153% on Day 3 and 207% on Day 7. This upregulation occurred in both levels of ω-3 and ω-6 PUFAs. One of the most abundant ω-6 PUFAs, arachidonic acid (20:4), displayed a significant and consistent upregulation of 490% from Day 3 onwards till Day 7. Representing ω-3 PUFAs, eicosapentaenoic acid (EPA, 20:5), docosapentaenoic acid (DPA, 22:5) and docosahexaenoic acid (DHA, 22:6) were also significantly upregulated by 628%, 261% and 213 on Day 7, respectively (Fig. 3-5B).

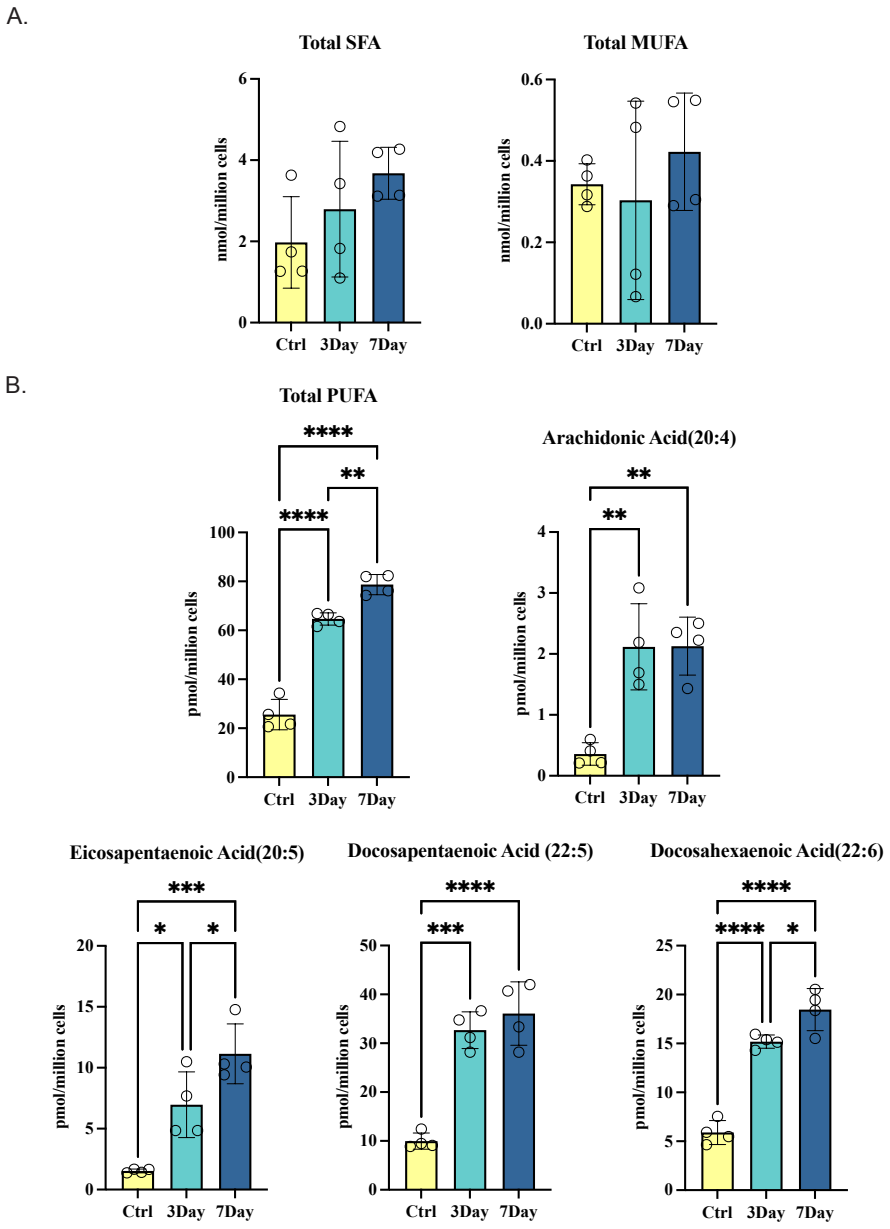

Figure 3-5. Changes of free fatty acids in senescent HUVECs.

*Saturated fatty acids exhibited an upregulation but with no significance (A left), and monounsaturated fatty acids did not display significant alterations in senescent HUVECs (A right), whereas the levels of polyunsaturated fatty acids (B) showed a substantial increase.Statistics were performed by ordinary one-way ANOVA with Prism 9, *p<0.05, **p<0.01, ***p<0.001, ****p<0.0001.*

3.3.6 Alteration of Cholesterol in EC Senescence

Given the critical role of free cholesterol in cellular structural and functional integrity, I also examined free cholesterol levels in senescent HUVECs. On Day 7, free cholesterol levels were upregulated by 85% (Fig. 3-6A). This change is significant to a membrane structural lipid. As up to 90% of free cholesterol is localised to the plasma membrane, it is noteworthy to further examine the PM cholesterol levels. To this end, I performed AmB resistance assay in non-senescent, early senescent and late senescent HUVECs. A notable cell death was found on day 7, indicating a marked increase in PM cholesterol levels between the transition from early to late senescence (Fig. 3-6B). This is consistent with the total cholesterol levels as quantified using lipidomics.

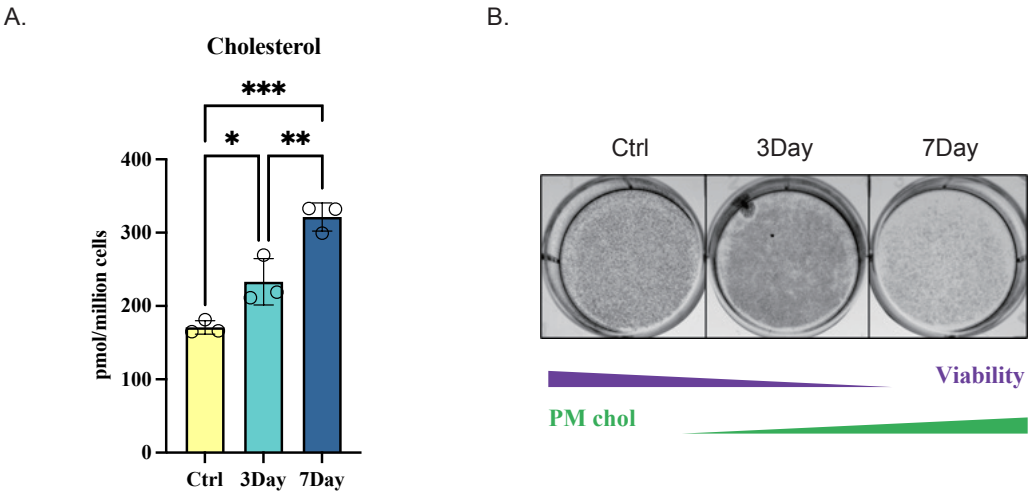

Figure 3-6. Alteration of cholesterol in senescent HUVECs.

*Levels of cholesterol were consistently upregulated in senescent HUVECs (A). AmphoB resistance test were performed with senescent HUVECs, and it appears that more cells were killed in late senescence compared to control, which indicated a lower level of PM cholesterol of senescent HUVECs. Statistics were performed by ordinary one-way ANOVA with Prism 9, *p<0.05, **p<0.01, ***p<0.001.*

3.3.7 ORP2 Expression in EC Senescence

Next, I further examined the expression of ORP2 in senescent HUVECs with western blotting and qPCR. In western blotting results, expression of ORP2, normalised to β-Actin, was significantly upregulated by 103% on Day 7 of senescence (Fig. 3-7A). This was associated with an increased expression of senescence marker p21 (Fig. 3-7A).

In line with ORP2 protein and PM cholesterol levels, I found that mRNA expression levels of ORP2 were also significantly increased during the transition from early to late senescence. On Day 7, the level of ORP2 mRNA was upregulated by 180% compared to non-senescent control (Fig. 3-7B).

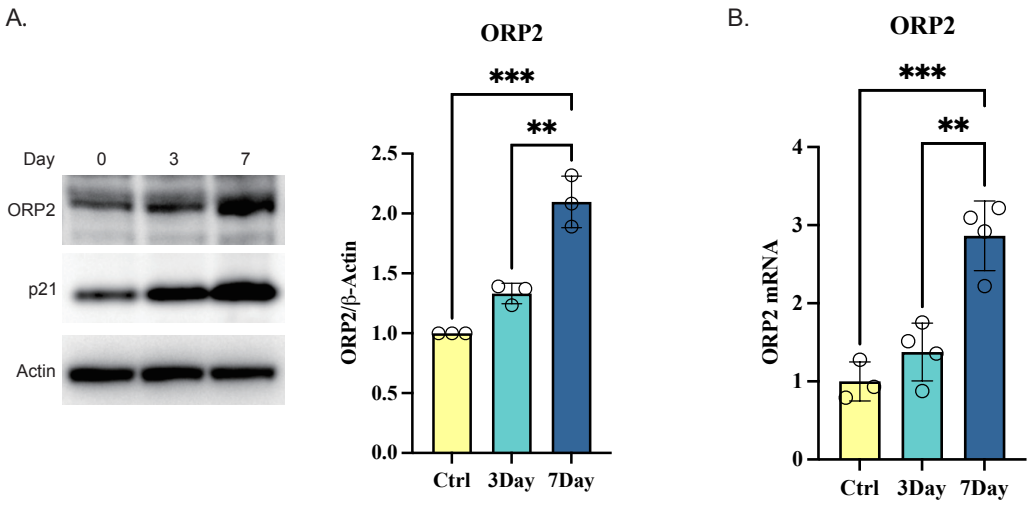

Figure 3-7. Changes of ORP2 expression in senescent HUVECs.

*Expression of ORP2 was found to be increased in both protein level of 100% on Day 7(A) and mRNA level of 200% on Day 7(B). Statistics were performed by ordinary one-way ANOVA with Prism 9, **p<0.01, ***p<0.001.*

3.3.8 Knockdown of ORP2 in EC Senescence

Having demonstrated an elevated ORP2 expression specifically in late senescent cells, I further investigated the impact of ORP2 senescence progression in HUVECs. Using lentiviral shRNA, I knocked down ORP2 on Day 3. Senescence was then assessed using SA-β-Gal staining on Day 7. ORP2-deficient HUVECs exhibited a dramatically reduced SA-β-Gal positivity, indicating that ORP2 deficiency suppressed senescence progression in HUVECs. (Fig. 3-8)

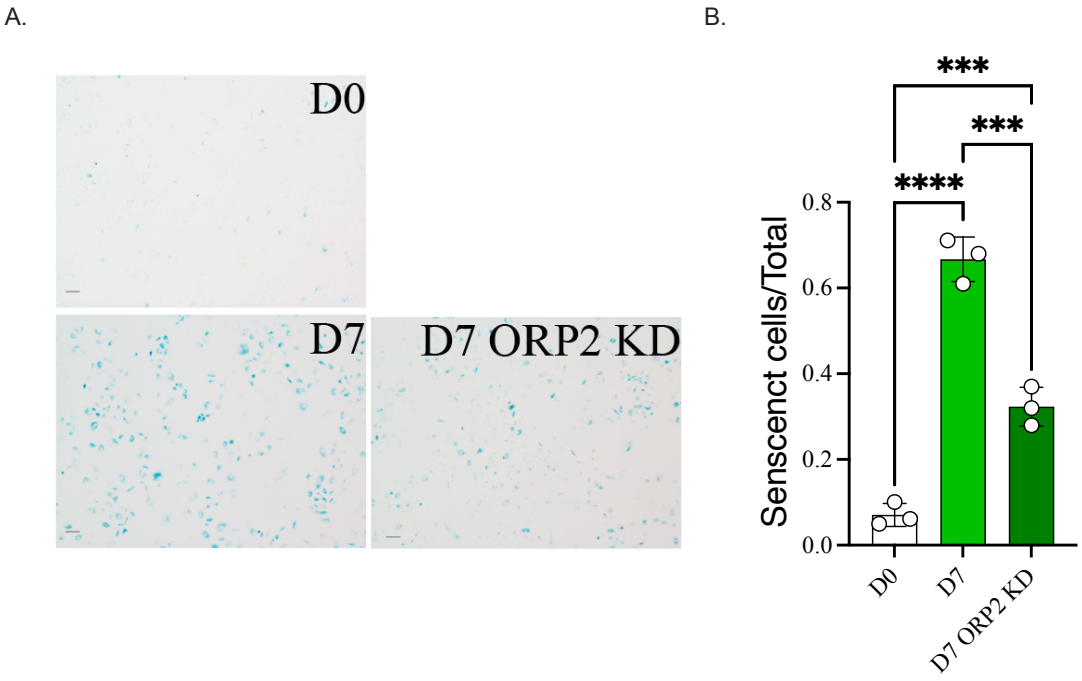

Figure 3-8. Deficiency of OPR2 suppresses progression of senescence in HUVECs.

*Lentiviral-shRNA knockdown of ORP2 was performed on the 3rd day after H2O2 stimulation, and it appears to be able to inhibit the generation of senescence in HUVECs, detected with SA-β-Gal staining (A) and quantified (B). Statistics were performed unpaired t-test with Prism 9, ***p<0.001, ****p<0.0001.*

3.4 Discussion

In this chapter, I found the alteration of lipids in the classes of sphingolipid (Fig. 3-2), glycerophospholipid (Fig. 3-3, Fig. 3-4), free fatty acids (Fig. 3-5) and cholesterol (Fig. 3-6A) in lipidomics analysis of H_2O_2 induced senescent HUVECs. The upregulation of cholesterol in senescent HUVECs occurs on PM (Fig. 3-6B). Additionally, intracellular cholesterol transporter ORP2 was found increased in EC senescence (Fig. 3-7), and deficiency of ORP2 can block the progress of senescence (Fig. 3-8).

The results of lipidomics in this study is from a combination of targeted and global lipidomics. Among the lipids have been shown in this chapter, sphingolipids, free fatty acids and cholesterol were detected with targeted lipidomics and the rest of them were detected in global lipidomics.

I found that ceramide was increased, and the well-known lipotoxic ceramide species d18:1/16:0 was significantly increased by 20%. Ceramide was earlier reported to be increased and able to promote replicative-stress senescence in fibroblasts [182] and endothelial cells [183]. Two subclasses of complex sphingolipids, sphingomyelin (SM) and hexosylceramide (HexCer), are firstly reported increased in endothelial senescence in this study. The primary function of sphingomyelin is to maintain cell membrane structure and especially the structure of lipid rafts [184]. The upregulation of SM in endothelial senescence might be related to SASP signalling. Upregualation of HexCer was reported in multiple diseases, such as Parkinson's disease [185],

Alzheimer's diseases [186], lung adenocarcinoma [187] and chronic kidney disease [188], but the function of HexCer is still not clear.

Phosphatidyleglycerol (PG), especially PG with polyunsaturated fatty acids, exhibits a continuing increase during the process of senescence. The major role of PG is the precursor of cardiolipin synthesis, and it is also relevant to cell signalling function and ion tunnels. Polyunsaturated PG is reported to be able to inhibit proliferation in mouse keratinocytes [189]. And PG can modify pattern recognition receptor signalling that is activated by toll-like receptors (TLR) and cell injury-associate signals [190-192]. Overall, the increase exhibits in levels of PUFA-PG might be a cause of proliferation arrest, however, on the other hand, the increase of total PG in EC senescence can also be considered as a self-protective effect under oxidise stress.

Phosphatifylinositol (PI) exhibits a fatty-acyl specific change during the progress of senescence. SFA/MUFA-containing PI exhibits downregulation while PUFA-containing PI exhibits an upregulation. An opposite change in PI was reported in p53-mutated cancer cells [193], in which SFA/MUFA-containing PI increased while PUFA-containing PI decreased. This might suggest that fatty acids composition in PI was suggested to be relevant to p53 regulation, and the remodelling of PI might be in response to proliferation regulation. The increase in cardiolipin was also observed, which indicates the accumulation of mitochondrias in senescent HUVECs

The levels of phosphatidylcholine and phosphatidylethanolamine were not altered in EC senescence, which is not surprising as they are the fundamental structural component of cellular membranes. However, PE-plasmalogen is exhibiting a massive upregulation during the progress. Plasmalogen can improve membrane dynamics during reparatory cycles, regulate signal transduction [137, 194] and act as secondary lipid messengers [137]. More importantly, plasmalogen serves as an antioxidant and protect other PUFA, phospholipid and lipoprotein from oxidative stress [194, 195]. In EC senescence, the upregulation of plasmalogen might be considered as a protective effect against oxidative stress delivered by the accumulation of mitochondria in senescent cells. The upregulation of plasmalogen has also been reported in cancers [196], but the mechanism of plasmalogen in diseases is still under studied.

In lysophospholipid, lysophosphatidylcholine (LPC) is the only class found to decrease. LPC is recognised to be able to promote and prolong endothelial activation [197], however, blood LPC level was reported to decrease with age in human body [198]. Low level of LPC was also reported in memory impairment in older adults [199] and in dementia [200].

The increase of ether-link LPC and LPE was found in EC senescence. The specific biofunction of them is not clear. In lipid metabolic pathways, LPCe and LPEe are precursors for plasmalogen [137]. The increase of LPCe and LPEe might be considered as upstream effect of increase of plasmalogens.

Other lysophospholipids, including LPG, LPS and LPI, also exhibit upregulation in senescence. Stimulation of LPG in vitro can promote migration and tube formation in HUVECs [201]; LPS and have been reported to negatively regulate immune response by the action of LPS G protein-coupled receptor on immune cells [202-204]. The mechanism of LPI is not clear.

Lysophospholipid analysis is based on global lipidomics data, but as their low abundance exists in endothelial cells, the number of detected species is not satisfied. In the future, lysophospholipid needs to be re-analysed with a targeted lipidomics method to expand the range of detection.

In free fatty acids, no significant change was found in saturated fatty acids and monounsaturated fatty acids, while PUFA demonstrated a dramatic increase in EC senescence. The upregulation of PUFA has been reported in other forms of senescence [205, 206]. The mechanism of increase of free PUFA is not clear, previous research indicates this is via the p38-dependent activation of phospholipase A2 to cleave PUFAs from membranes [207]. And the desaturation of PUFA is reported to be relevant with glycolytic NAD^+ recycling to neutralise oxidative stress. Further mechanism study is required to understand this role of PUFA in senescence.

In senescent cells, apart from the cell cycle arrest biomarkers and the changes in the lysosome, the alteration of cellular morphology [208-210], which means the senescent cells are enlarged, flattened and multinucleated [209, 211]. And this morphological change can also be observed in tissues

[210]. Considering the changes in the membranal structural lipids such as the phospholipids, sphingomyelin and cholesterol, this should be relevant to the change of cellular morphology, as the composition of membranal lipids tightly regulates the curvature and fluidity of the membrane [212].

Additionally, I found the level of free cholesterol increased in EC senescence and the PM cholesterol level increased as well. The role of intracellular cholesterol in EC senescence is unstudied. The expression of ORP2 in senescent HUVECs was unregulated in both protein level and mRNA levels.

Due to the morphological alterations and inflammatory phenotype associated with cellular senescence, cholesterol, being a crucial component in both senescence mechanisms, has become the primary lipid species of interest in my study. Therefore, I conducted ORP2 knockdown in senescent HUVECs to find potential links between PM cholesterol and EC senescence. Interestingly, knockdown ORP2 in the early stage of senescence successfully block the progression of senescence.

With the limitation of time, I could not continue to investigate further effects and mechanisms in terms of inhibition of senescence.

Overall, this chapter of endothelial senescence lipid profiling study reveals the alteration of intracellular lipids in senescent HUVECs. Dramatic changes were found in the classes of sphingolipid, phospholipid, free fatty acid and cholesterol. Lipid profiling gives potential lipid target in study of senescence.

The inhibition of senescence by ORP2 knockdown suggests the importance of intracellular cholesterol transport in EC senescence.

For future work, the first thing that I will continue with is to expand the profile of endothelial senescence lipidomes. This will include other form of senescence and more lipid species such as oxidised lipids. On the other hand, I will further investigate the role of ORP2 in senescence. Additional senescent markers and SASP markers in the context of ORP2 deficiency will be examined. Based on the ApoE/ORP2-EKO double knockout mice aforementioned, in vivo studies involving animal models can provide valuable insights into the physiological consequences of ORP2 deficiency and its impact on senescence-related processes in cardiovascular disease.

Chapter 4. Conclusion

This thesis is composed of two topics focusing on endothelial activation and endothelial senescence.

In chapter 2, I found an anti-inflammation effect of ORP2 knockdown in endothelial cells. The main findings of Chapter 2 are listed below:

1. I found the knockdown of ORP2 can reduce PM cholesterol level in HUVECs.
2. Knockdown of ORP2 can inhibit activation of NFκB and NLRP3-inflammasome in endothelial activation.
3. Knockdown of ORP2 can inhibit the expression of adhesion molecules and the recruitment of monocytes in endothelial activation.
4. Knockdown of ORP2 does not alter the expression of lipid rafts structural proteins, Flot-1 and Cav-1.

My results reveal the role of ORP2 in endothelial activation and subsequent inflammatory action. These provide insights of role of intracellular cholesterol in atherosclerosis and offer a potential target in CVD treatment and drug development.

In chapter 3, I conducted lipidomics analysis with senescent HUVECs. Based on the alteration of cholesterol, I further examine the expression of ORP2 in senescent HUVEC and conduct ORP2 knockdown in early stage of senescent HUVEC. The main findings in this chapter are listed below:

1. Sphingolipids, including ceramides, sphingomyelins, and hexosylceramides are found upregulated in EC senescence.
2. Phospholipid exhibits alteration in EC senescence. PG, PUFA-PI, PUFA-CLS, PEp, LPS, LPI, LPG, ether-linked LPC and ether-linked LPE are increased, while FSA/MUFA-PI and LPC are decreased.
3. PUFA exhibits an extradentary upregulation, while SFA and MUFA are with no significant changes.
4. Cholesterol and especially PM cholesterol is found increased in EC senescence.
5. Expression of ORP2 in EC senescence increases in both protein and mRNA levels.
6. Knockdown of ORP2 can block the progression of senescence.

My results can provide key information of lipid alteration in EC senescence for studies on functions of lipids in EC senescence and CVD. Additionally, it reveals that ORP2 also plays an important role in senescence.

Reference list

1. WILSON, S.H. and A. LERMAN, *Function of vascular endothelium*, in *Heart physiology and pathophysiology*. 2001, Elsevier. p. 473-480.

2. Schechter, A.N. and M.T. Gladwin, *Hemoglobin and the paracrine and endocrine functions of nitric oxide.* New England Journal of Medicine, 2003. **348**(15): p. 1483-1485.

3. Deanfield, J.E., J.P. Halcox, and T.J. Rabelink, *Endothelial function and dysfunction: testing and clinical relevance.* Circulation, 2007. **115**(10): p. 1285-1295.

4. Furchgott, R.F. and J.V. Zawadzki, *The obligatory role of endothelial cells in the relaxation of arterial smooth muscle by acetylcholine.* nature, 1980. **288**(5789): p. 373-376.

5. Forstermann, U. and T. Münzel, *Endothelial nitric oxide synthase in vascular disease: from marvel to menace.* Circulation, 2006. **113**(13): p. 1708-1714.

6. Denninger, J.W. and M.A. Marletta, *Guanylate cyclase and the .NO/cGMP signaling pathway.* Biochimica Et Biophysica Acta, 1999. **1411**(2-3): p. 334-350.

7. Surks, H.K., et al., *Regulation of myosin phosphatase by a specific interaction with cGMP- dependent protein kinase Ialpha.* Science (New York, N.Y.), 1999. **286**(5444): p. 1583-1587.

8. Stamler, J.S., S. Lamas, and F.C. Fang, *Nitrosylation: the prototypic redox-based signaling mechanism.* Cell, 2001. **106**(6): p. 675-683.

9. Ghosh, S. and M. Karin, *Missing pieces in the NF-κB puzzle.* cell, 2002. **109**(2): p. S81-S96.

10. Hess, D.T. and J.S. Stamler, *Regulation by S-nitrosylation of protein post-translational modification.* The Journal of Biological Chemistry, 2012. **287**(7): p. 4411-4418.

11. Kang-Decker, N., et al., *Nitric oxide promotes endothelial cell survival signaling through S-nitrosylation and activation of dynamin-2.* Journal of cell science, 2007. **120**(3): p. 492-501.

12. Ignarro, L.J., et al., *Role of the arginine-nitric oxide pathway in the regulation of vascular smooth muscle cell proliferation.* Proceedings of the National Academy of Sciences, 2001. **98**(7): p. 4202-4208.

13. Matsushita, K., et al., *Nitric oxide regulates exocytosis by S-nitrosylation of N-ethylmaleimide-sensitive factor.* Cell, 2003. **115**(2): p. 139-150.

14. Corson, M.A., et al., *Phosphorylation of endothelial nitric oxide synthase in response to fluid shear stress.* Circulation research, 1996. **79**(5): p. 984-991.

15. Govers, R. and T.J. Rabelink, *Cellular regulation of endothelial nitric oxide synthase.* American Journal of Physiology-Renal Physiology, 2001. **280**(2): p. F193-F206.

16. Moncada, S., E. Higgs, and J. Vane, *Human arterial and venous tissues generate prostacyclin (prostaglandin x), a potent inhibitor of platelet aggregation.* The Lancet, 1977. **309**(8001): p. 18-21.

17. Dorris, S.L. and R.S. Peebles, *PGI2 as a regulator of inflammatory diseases.* Mediators of Inflammation, 2012. **2012**: p. 926968.

18. Hansson, G.K., *Inflammation, atherosclerosis, and coronary artery disease.* New England journal of medicine, 2005. **352**(16): p. 1685-1695.

19. Rhee, S.G., *H2O2, a necessary evil for cell signaling.* Science, 2006. **312**(5782): p. 1882-1883.

20. Yang, Y.-M., et al., *eNOS uncoupling and endothelial dysfunction in aged vessels.* American Journal of Physiology-Heart and Circulatory Physiology, 2009. **297**(5): p. H1829-H1836.

21. Majno, G., *Ultrastructure of the vascular membrane.* Hanbook of Physiology Sect, 1965(11): p. 2293-2375.

22. Cotran, R., *The fine structure of the microvasculature in relation to normal and altered permeability.* Physical bases of circulatory transport: Regulation and exchange, 1967. **15**: p. 249-275.

23. Pober, J.S. and R.S. Cotran, *The role of endothelial cells in inflammation.* Transplantation, 1990. **50**(4): p. 537-544.

24. Pober, J.S. and R.S. Cotran, *Cytokines and endothelial cell biology.* Physiological reviews, 1990. **70**(2): p. 427-451.

25. Pober, J.S. and W.C. Sessa, *Evolving functions of endothelial cells in inflammation.* Nature Reviews Immunology, 2007. **7**(10): p. 803-815.

26. Barreiro, O., et al., *Dynamic interaction of VCAM-1 and ICAM-1 with moesin and ezrin in a novel endothelial docking structure for adherent leukocytes.* The Journal of cell biology, 2002. **157**(7): p. 1233-1245.

27. Rollins, B., et al., *Cytokine-activated human endothelial cells synthesize and secrete a monocyte chemoattractant, MCP-1/JE.* The American journal of pathology, 1990. **136**(6): p. 1229.

28. Pober, J.S. and M.A. Gimbrone, *Expression of Ia-like antigens by human vascular endothelial cells is inducible in vitro: demonstration by monoclonal antibody binding and immunoprecipitation.* Proceedings of the National Academy of Sciences, 1982. **79**(21): p. 6641-6645.

29. Cotran, R.S., et al., *Induction and detection of a human endothelial activation antigen in vivo.* The Journal of experimental medicine, 1986. **164**(2): p. 661-666.

30. Collins, T. and M.I. Cybulsky, *NF-κB: pivotal mediator or innocent bystander in atherogenesis?* The Journal of clinical investigation, 2001. **107**(3): p. 255-264.

31. Bui, T.M., H.L. Wiesolek, and R. Sumagin, *ICAM-1: A master regulator of cellular responses in inflammation, injury resolution, and tumorigenesis.* Journal of Leukocyte Biology, 2020. **108**(3): p. 787-799.

32. Groves, R.W., et al., *Endothelial leucocyte adhesion molecule-1 (ELAM-1) expression in cutaneous inflammation.* The British Journal of Dermatology, 1991. **124**(2): p. 117-123.

33. Elices, M.J., et al., *VCAM-1 on activated endothelium interacts with the leukocyte integrin VLA-4 at a site distinct from the VLA-4/fibronectin binding site.* Cell, 1990. **60**(4): p. 577-584.

34. Nakashima, Y., et al., *Upregulation of VCAM-1 and ICAM-1 at atherosclerosis-prone sites on the endothelium in the ApoE-deficient mouse.* Arteriosclerosis, thrombosis, and vascular biology, 1998. **18**(5): p. 842-851.

35. Brown, J.D., et al., *NF-κB directs dynamic super enhancer formation in inflammation and atherogenesis.* Molecular cell, 2014. **56**(2): p. 219-231.

36. Harjunpää, H., et al., *Cell Adhesion Molecules and Their Roles and Regulation in the Immune and Tumor Microenvironment.* Frontiers In Immunology, 2019. **10**: p. 1078.

37. Cavallaro, U. and E. Dejana, *Adhesion molecule signalling: not always a sticky business.* Nature Reviews. Molecular Cell Biology, 2011. **12**(3): p. 189-197.

38. Cybulsky, M.I. and M.A. Gimbrone Jr, *Endothelial expression of a mononuclear leukocyte adhesion molecule during atherogenesis.* Science, 1991. **251**(4995): p. 788-791.

39. O'Brien, K.D., et al., *Vascular cell adhesion molecule-1 is expressed in human coronary atherosclerotic plaques. Implications for the mode of progression of advanced coronary atherosclerosis.* The Journal of clinical investigation, 1993. **92**(2): p. 945-951.

40. Li, H., et al., *An atherogenic diet rapidly induces VCAM-1, a cytokine-regulatable mononuclear leukocyte adhesion molecule, in rabbit aortic endothelium.* Arteriosclerosis and thrombosis: a journal of vascular biology, 1993. **13**(2): p. 197-204.

41. Wee, H., et al., *ICAM-1/LFA-1 interaction contributes to the induction of endothelial cell-cell separation: implication for enhanced leukocyte diapedesis.* Experimental & Molecular Medicine, 2009. **41**(5): p. 341-348.

42. Purdy, M., et al., *P- and E- selectin in venous thrombosis and non-venous pathologies.* Journal of Thrombosis and Haemostasis : JTH, 2022. **20**(5): p. 1056-1066.

43. McEver, R.P., *Selectins: initiators of leucocyte adhesion and signalling at the vascular wall.* Cardiovascular Research, 2015. **107**(3): p. 331-339.

44. De Caterina, R., et al., *Soluble vascular cell adhesion molecule-1 as a biohumoral correlate of atherosclerosis.* Arteriosclerosis, thrombosis, and vascular biology, 1997. **17**(11): p. 2646-2654.

45. Bittar, L.F., et al., *Increased inflammation and endothelial markers in patients with late severe post-thrombotic syndrome.* PloS One, 2020. **15**(1): p. e0227150.

46. Hansson, G.K., *Immune mechanisms in atherosclerosis.* Arteriosclerosis, thrombosis, and vascular biology, 2001. **21**(12): p. 1876-1890.

47. Eid, R.E., et al., *Interleukin-17 and interferon-γ are produced concomitantly by human coronary artery–infiltrating T cells and act synergistically on vascular smooth muscle cells.* Circulation, 2009. **119**(10): p. 1424-1432.

48. Chen, Z., et al., *Endothelial dysfunction: the role of sterol regulatory element-binding protein-induced NOD-like receptor family pyrin domain-containing protein 3 inflammasome in atherosclerosis.* Current opinion in lipidology, 2014. **25**(5): p. 339-349.

49. Mangan, M.S., et al., *Targeting the NLRP3 inflammasome in inflammatory diseases.* Nature reviews Drug discovery, 2018. **17**(8): p. 588-606.

50. Shi, J., W. Gao, and F. Shao, *Pyroptosis: gasdermin-mediated programmed necrotic cell death.* Trends in biochemical sciences, 2017. **42**(4): p. 245-254.

51. Bergsbaken, T., S.L. Fink, and B.T. Cookson, *Pyroptosis: host cell death and inflammation.* Nature Reviews. Microbiology, 2009. **7**(2).

52. Higashi, Y., *Roles of oxidative stress and inflammation in vascular endothelial dysfunction-related disease.* Antioxidants, 2022. **11**(10): p. 1958.

53. Mäki-Petäjä, K.M., et al., *Ezetimibe and simvastatin reduce inflammation, disease activity, and aortic stiffness and improve endothelial function in rheumatoid arthritis.* Journal of the American College of Cardiology, 2007. **50**(9): p. 852-858.

54. Kotani, K., M. Miyamoto, and H. Ando, *The effect of treatments for rheumatoid arthritis on endothelial dysfunction evaluated by flow-mediated vasodilation in patients with rheumatoid arthritis.* Current vascular pharmacology, 2017. **15**(1): p. 10-18.

55. Pacholczak-Madej, R., et al., *Endothelial dysfunction in patients with systemic sclerosis.* Advances in Dermatology and Allergology/Postępy Dermatologii i Alergologii, 2020. **37**(4): p. 495-502.

56. Wen, Y., et al., *Ultrasound evaluation of endothelial dysfunction in immunoglobulin-resistant children with acute Kawasaki disease.* Clinical Rheumatology, 2022. **41**(12): p. 3797-3805.

57. Becker, L., et al., *Endothelial dysfunction assessed by brachial artery ultrasound in severe sepsis and septic shock.* Journal of critical care, 2012. **27**(3): p. 316. e9-316. e14.

58. Swanson, K.V., M. Deng, and J.P.Y. Ting, *The NLRP3 inflammasome: molecular activation and regulation to therapeutics.* Nature Reviews. Immunology, 2019. **19**(8): p. 477-489.

59. Hayflick, L., *THE LIMITED IN VITRO LIFETIME OF HUMAN DIPLOID CELL STRAINS.* Experimental Cell Research, 1965. **37**: p. 614-636.

60. Bloom, S.I., et al., *Mechanisms and consequences of endothelial cell senescence.* Nature Reviews. Cardiology, 2023. **20**(1): p. 38-51.

61. Childs, B.G., et al., *Senescence and apoptosis: dueling or complementary cell fates?* EMBO reports, 2014. **15**(11): p. 1139-1153.

62. Donato, A.J., D.R. Machin, and L.A. Lesniewski, *Mechanisms of dysfunction in the aging vasculature and role in age-related disease.* Circulation Research, 2018. **123**(7): p. 825-848.

63. Lähteenvuo, J. and A. Rosenzweig, *Effects of aging on angiogenesis.* Circulation research, 2012. **110**(9): p. 1252-1264.

64. Krouwer, V.J., et al., *Endothelial cell senescence is associated with disrupted cell-cell junctions and increased monolayer permeability.* Vascular cell, 2012. **4**(1): p. 1-10.

65. Pérez-Rivero, G., et al., *Mice deficient in telomerase activity develop hypertension because of an excess of endothelin production.* Circulation, 2006. **114**(4): p. 309-317.

66. Childs, B.G., et al., *Senescent intimal foam cells are deleterious at all stages of atherosclerosis.* Science, 2016. **354**(6311): p. 472-477.

67. Yanaka, M., et al., *Increased monocytic adhesion by senescence in human umbilical vein endothelial cells.* Bioscience, biotechnology, and biochemistry, 2011. **75**(6): p. 1098-1103.

68. Gevaert, A.B., et al., *Endothelial senescence contributes to heart failure with preserved ejection fraction in an aging mouse model.* Circulation: Heart Failure, 2017. **10**(6): p. e003806.

69. Mallat, Z., et al., *Elevated levels of shed membrane microparticles with procoagulant potential in the peripheral circulating blood of patients with acute coronary syndromes.* Circulation, 2000. **101**(8): p. 841-843.

70. Rajagopalan, S., et al., *Endothelial cell apoptosis in systemic lupus erythematosus: a common pathway for abnormal vascular function and thrombosis propensity.* Blood, 2004. **103**(10): p. 3677-3683.

71. Chala, N., et al., *Mechanical fingerprint of senescence in endothelial cells.* Nano Letters, 2021. **21**(12): p. 4911-4920.

72. Campisi, J. and F. d'Adda di Fagagna, *Cellular senescence: when bad things happen to good cells.* Nature reviews Molecular cell biology, 2007. **8**(9): p. 729-740.

73. Donato, A.J., et al., *Cellular and molecular biology of aging endothelial cells.* Journal of molecular and cellular cardiology, 2015. **89**: p. 122-135.

74. Lee, B.Y., et al., *Senescence-associated β-galactosidase is lysosomal β-galactosidase.* Aging cell, 2006. **5**(2): p. 187-195.

75. Kohli, J., et al., *Algorithmic assessment of cellular senescence in experimental and clinical specimens.* Nature protocols, 2021. **16**(5): p. 2471-2498.

76. Basisty, N., et al., *A proteomic atlas of senescence-associated secretomes for aging biomarker development.* PLoS biology, 2020. **18**(1): p. e3000599.

77. Coppé, J.-P., et al., *The senescence-associated secretory phenotype: the dark side of tumor suppression.* Annual review of pathology: mechanisms of disease, 2010. **5**: p. 99-118.

78. Lafargue, A., et al., *Ionizing radiation induces long-term senescence in endothelial cells through mitochondrial respiratory complex II dysfunction and superoxide generation.* Free Radical Biology and Medicine, 2017. **108**: p. 750-759.

79. Donato, A.J., et al., *Direct evidence of endothelial oxidative stress with aging in humans: relation to impaired endothelium-dependent dilation and upregulation of nuclear factor-κB.* Circulation research, 2007. **100**(11): p. 1659-1666.

80. Yin, Y., et al., *Vascular endothelial cells senescence is associated with NOD-like receptor family pyrin domain-containing 3 (NLRP3) inflammasome activation via reactive oxygen species (ROS)/thioredoxin-interacting protein (TXNIP) pathway.* The International Journal of Biochemistry & Cell Biology, 2017. **84**: p. 22-34.

81. Khan, S.Y., et al., *Premature senescence of endothelial cells upon chronic exposure to TNFα can be prevented by N-acetyl cysteine and plumericin.* Scientific Reports, 2017. **7**(1): p. 39501.

82. Coleman, P.R., et al., *Age-associated stresses induce an anti-inflammatory senescent phenotype in endothelial cells.* Aging (Albany NY), 2013. **5**(12): p. 913.

83. Goldstein, J.L., R.A. DeBose-Boyd, and M.S. Brown, *Protein sensors for membrane sterols.* Cell, 2006. **124**(1): p. 35-46.

84. Ikonen, E., *Cellular cholesterol trafficking and compartmentalization.* Nature reviews Molecular cell biology, 2008. **9**(2): p. 125-138.

85. Iuliano, L., *Pathways of cholesterol oxidation via non-enzymatic mechanisms.* Chemistry and Physics of Lipids, 2011. **164**(6): p. 457-468.

86. Lange, Y., et al., *Regulation of endoplasmic reticulum cholesterol by plasma membrane cholesterol.* Journal of Lipid Research, 1999. **40**(12): p. 2264-2270.

87. Luo, J., H. Yang, and B.-L. Song, *Mechanisms and regulation of cholesterol homeostasis.* Nature Reviews. Molecular Cell Biology, 2020. **21**(4): p. 225-245.

88. Howell, G.J., et al., *Cell biology of membrane trafficking in human disease.* International Review of Cytology, 2006. **252**.

89. Olkkonen, V.M. and E. Ikonen, *Cholesterol transport in the late endocytic pathway: Roles of ORP family proteins.* The Journal of steroid biochemistry and molecular biology, 2022. **216**: p. 106040.

90. Pfisterer, S.G., J. Peränen, and E. Ikonen, *LDL–cholesterol transport to the endoplasmic reticulum: current concepts.* Current opinion in lipidology, 2016. **27**(3): p. 282.

91. Mesmin, B. and F.R. Maxfield, *Intracellular sterol dynamics.* Biochimica et Biophysica Acta (BBA)-Molecular and Cell Biology of Lipids, 2009. **1791**(7): p. 636-645.

92. Chu, B.-B., et al., *Cholesterol transport through lysosome-peroxisome membrane contacts.* Cell, 2015. **161**(2): p. 291-306.

93. Scorrano, L., et al., *Coming together to define membrane contact sites.* Nature communications, 2019. **10**(1): p. 1-11.

94. Eden, E.R., et al., *Annexin A1 tethers membrane contact sites that mediate ER to endosome cholesterol transport.* Developmental cell, 2016. **37**(5): p. 473-483.

95. Wong, L.H., E.R. Eden, and C.E. Futter, *Roles for ER: endosome membrane contact sites in ligand-stimulated intraluminal vesicle formation.* Biochemical Society Transactions, 2018. **46**(5): p. 1055-1062.

96. Kanerva, K., et al., *LDL cholesterol recycles to the plasma membrane via a Rab8a-Myosin5b-actin-dependent membrane transport route.* Developmental cell, 2013. **27**(3): p. 249-262.

97. van den Boomen, D.J., et al., *A trimeric Rab7 GEF controls NPC1-dependent lysosomal cholesterol export.* Nature communications, 2020. **11**(1): p. 1-18.

98. Johansson, M., et al., *The oxysterol-binding protein homologue ORP1L interacts with Rab7 and alters functional properties of late endocytic compartments.* Molecular biology of the cell, 2005. **16**(12): p. 5480-5492.

99. Lingwood, D. and K. Simons, *Lipid rafts as a membrane-organizing principle.* Science (New York, N.Y.), 2010. **327**(5961): p. 46-50.

100. Legler, D.F., et al., *Recruitment of TNF receptor 1 to lipid rafts is essential for TNFalpha-mediated NF-kappaB activation.* Immunity, 2003. **18**(5): p. 655-664.

101. Goicoechea, L., et al., *Mitochondrial cholesterol: Metabolism and impact on redox biology and disease.* Redox Biology, 2023: p. 102643.

102. Solsona-Vilarrasa, E., et al., *Cholesterol enrichment in liver mitochondria impairs oxidative phosphorylation and disrupts the assembly of respiratory supercomplexes.* Redox biology, 2019. **24**: p. 101214.

103. Bosch, M., et al., *Caveolin-1 deficiency causes cholesterol-dependent mitochondrial dysfunction and apoptotic susceptibility.* Current Biology, 2011. **21**(8): p. 681-686.

104. Sheedy, F.J., et al., *CD36 coordinates NLRP3 inflammasome activation by facilitating intracellular nucleation of soluble ligands into particulate ligands in sterile inflammation.* Nature immunology, 2013. **14**(8): p. 812-820.

105. Tall, A.R. and M. Westerterp, *Inflammasomes, neutrophil extracellular traps, and cholesterol.* Journal of lipid research, 2019. **60**(4): p. 721-727.

106. Kentala, H., M. Weber-Boyvat, and V.M. Olkkonen, *OSBP-related protein family: mediators of lipid transport and signaling at membrane contact sites.* International review of cell and molecular biology, 2016. **321**: p. 299-340.

107. Pietrangelo, A. and N.D. Ridgway, *Bridging the molecular and biological functions of the oxysterol-binding protein family.* Cellular and Molecular Life Sciences, 2018. **75**(17): p. 3079-3098.

108. de Saint-Jean, M., et al., *Osh4p exchanges sterols for phosphatidylinositol 4-phosphate between lipid bilayers.* Journal of Cell Biology, 2011. **195**(6): p. 965-978.

109. Mesmin, B., et al., *A four-step cycle driven by PI (4) P hydrolysis directs sterol/PI (4) P exchange by the ER-Golgi tether OSBP.* Cell, 2013. **155**(4): p. 830-843.

110. Chung, J., et al., *PI4P/phosphatidylserine countertransport at ORP5-and ORP8-mediated ER–plasma membrane contacts.* Science, 2015. **349**(6246): p. 428-432.

111. Moser von Filseck, J., et al., *Phosphatidylserine transport by ORP/Osh proteins is driven by phosphatidylinositol 4-phosphate.* Science, 2015. **349**(6246): p. 432-436.

112. Von Filseck, J.M., et al., *A phosphatidylinositol-4-phosphate powered exchange mechanism to create a lipid gradient between membranes.* Nature communications, 2015. **6**(1): p. 1-12.

113. Ngo, M.H., T.R. Colbourne, and N.D. Ridgway, *Functional implications of sterol transport by the oxysterol-binding protein gene family.* The Biochemical Journal, 2010. **429**(1): p. 13-24.

114. Johansson, M., et al., *The two variants of oxysterol binding protein-related protein-1 display different tissue expression patterns, have different intracellular localization, and are functionally distinct.* Molecular biology of the cell, 2003. **14**(3): p. 903-915.

115. Rocha, N., et al., *Cholesterol sensor ORP1L contacts the ER protein VAP to control Rab7–RILP–p150Glued and late endosome positioning.* Journal of Cell Biology, 2009. **185**(7): p. 1209-1225.

116. Du, X., et al., *A role for oxysterol-binding protein–related protein 5 in endosomal cholesterol trafficking.* Journal of Cell Biology, 2011. **192**(1): p. 121-135.

117. Ghai, R., et al., *ORP5 and ORP8 bind phosphatidylinositol-4, 5-biphosphate (PtdIns (4, 5) P 2) and regulate its level at the plasma membrane.* Nature communications, 2017. **8**(1): p. 1-14.

118. Laitinen, S., et al., *ORP2, a homolog of oxysterol binding protein, regulates cellular cholesterol metabolism.* Journal of lipid research, 2002. **43**(2): p. 245-255.

119. Hynynen, R., et al., *Overexpression of OSBP-related protein 2 (ORP2) induces changes in cellular cholesterol metabolism and enhances endocytosis.* Biochemical journal, 2005. **390**(1): p. 273-283.

120. Hynynen, R., et al., *OSBP-related protein 2 is a sterol receptor on lipid droplets that regulates the metabolism of neutral lipids [S].* Journal of lipid research, 2009. **50**(7): p. 1305-1315.

121. Wang, H., et al., *ORP2 delivers cholesterol to the plasma membrane in exchange for phosphatidylinositol 4, 5-bisphosphate (PI (4, 5) P2).* Molecular cell, 2019. **73**(3): p. 458-473. e7.

122. Koponen, A., et al., *ORP2 interacts with phosphoinositides and controls the subcellular distribution of cholesterol.* Biochimie, 2019. **158**: p. 90-101.

123. Kentala, H., et al., *OSBP-related protein-2 (ORP2): a novel Akt effector that controls cellular energy metabolism.* Cellular and Molecular Life Sciences, 2018. **75**(21): p. 4041-4057.

124. Kentala, H., et al., *Analysis of ORP2 -knockout hepatocytes uncovers a novel function in actin cytoskeletal regulation.* The FASEB Journal, 2018. **32**(3): p. 1281-1295.

125. Weber-Boyvat, M., et al., *Ligand-dependent localization and function of ORP–VAP complexes at membrane contact sites.* Cellular and molecular life sciences, 2015. **72**(10): p. 1967-1987.

126. Wang, T., et al., *OSBPL2 Is Required for the Binding of COPB1 to ATGL and the Regulation of Lipid Droplet Lipolysis.* IScience, 2020. **23**(7): p. 101252.

127. Wang, T., et al., *Oxysterol-binding protein-like 2 contributes to the developmental progression of preadipocytes by binding to β-catenin.* Cell Death Discovery, 2021. **7**(1): p. 109.

128. Shi, H., et al., *Mutations in OSBPL2 cause hearing loss associated with primary cilia defects via sonic hedgehog signaling.* JCI insight, 2022. **7**(4).

129. Koponen, A., et al., *ORP2, a cholesterol transporter, regulates angiogenic signaling in endothelial cells.* The FASEB Journal, 2020. **34**(11): p. 14671-14694.

130. Kishimoto, K., et al., *Nondestructive quantification of neutral lipids by thin-layer chromatography and laser-fluorescent scanning: suitable methods for "lipidome" analysis.* Biochemical and biophysical research communications, 2001. **281**(3): p. 657-662.

131. Fahy, E., et al., *Update of the LIPID MAPS comprehensive classification system for lipids.* Journal of Lipid Research, 2009. **50 Suppl**(Suppl): p. S9-14.

132. Merrill, A.H., et al., *Sphingolipidomics: a valuable tool for understanding the roles of sphingolipids in biology and disease.* Journal of Lipid Research, 2009. **50**: p. S97-S102.

133. Gault, C.R., L.M. Obeid, and Y.A. Hannun, *An overview of sphingolipid metabolism: from synthesis to breakdown.* Sphingolipids as signaling and regulatory molecules, 2010: p. 1-23.

134. Shindou, H. and T. Shimizu, *Acyl-CoA: lysophospholipid acyltransferases.* Journal of biological chemistry, 2009. **284**(1): p. 1-5.

135. Yang, K., et al., *Shotgun lipidomics identifies a paired rule for the presence of isomeric ether phospholipid molecular species.* PloS one, 2007. **2**(12): p. e1368.

136. Fagone, P. and S. Jackowski, *Membrane phospholipid synthesis and endoplasmic reticulum function.* Journal of lipid research, 2009. **50**: p. S311-S316.

137. Nagan, N. and R.A. Zoeller, *Plasmalogens: biosynthesis and functions.* Progress in lipid research, 2001. **40**(3): p. 199-229.

138. McMahon, H.T. and E. Boucrot, *Membrane curvature at a glance.* Journal of cell science, 2015. **128**(6): p. 1065-1070.

139. Han, X., *Lipidomics for studying metabolism.* Nature Reviews. Endocrinology, 2016. **12**(11): p. 668-679.

140. Schaffer, J.E., *Lipotoxicity: when tissues overeat.* Current opinion in lipidology, 2003. **14**(3): p. 281-287.

141. Kohlwein, S.D., M. Veenhuis, and I.J. van der Klei, *Lipid droplets and peroxisomes: key players in cellular lipid homeostasis or a matter of fat—store'em up or burn'em down.* Genetics, 2013. **193**(1): p. 1-50.

142. Jackson, C.L., *Lipid droplet biogenesis.* Current Opinion in Cell Biology, 2019. **59**: p. 88-96.

143. Henne, W.M., M.L. Reese, and J.M. Goodman, *The assembly of lipid droplets and their roles in challenged cells.* The EMBO journal, 2018. **37**(12): p. e98947.

144. Carrasco, S. and I. Mérida, *Diacylglycerol, when simplicity becomes complex.* Trends In Biochemical Sciences, 2007. **32**(1): p. 27-36.

145. Poursharifi, P., S.R.M. Madiraju, and M. Prentki, *Monoacylglycerol signalling and ABHD6 in health and disease.* Diabetes, Obesity & Metabolism, 2017. **19 Suppl 1**: p. 76-89.

146. Han, X. and R.W. Gross, *Global analyses of cellular lipidomes directly from crude extracts of biological samples by ESI mass spectrometry: a bridge to lipidomics.* Journal of lipid research, 2003. **44**(6): p. 1071-1079.

147. Lee, S.H., et al., *Targeted lipidomics using electron capture atmospheric pressure chemical ionization mass spectrometry.* Rapid Communications in Mass Spectrometry, 2003. **17**(19): p. 2168-2176.

148. Wang, R., et al., *Integration of lipidomics and metabolomics for in-depth understanding of cellular mechanism and disease progression.* Journal of genetics and genomics, 2020. **47**(2): p. 69-83.

149. Kyle, J.E., *Extracting biological insight from untargeted lipidomics data.* Computational Methods and Data Analysis for Metabolomics, 2020: p. 121-137.

150. Kim, W.S., et al., *Lipidomics analysis of behavioral variant frontotemporal dementia: a scope for biomarker development.* Frontiers in neurology, 2018. **9**: p. 104.

151. Seah, J.Y.H., et al., *Plasma sphingolipids and risk of cardiovascular diseases: a large-scale lipidomic analysis.* Metabolomics, 2020. **16**: p. 1-12.

152. Taguchi, R. and M. Ishikawa, *Precise and global identification of phospholipid molecular species by an Orbitrap mass spectrometer and automated search engine Lipid Search.* Journal of Chromatography. A, 2010. **1217**(25): p. 4229-4239.

153. Cajka, T. and O. Fiehn, *Comprehensive analysis of lipids in biological systems by liquid chromatography-mass spectrometry.* TrAC Trends in Analytical Chemistry, 2014. **61**: p. 192-206.

154. Cajka, T. and O. Fiehn, *Toward merging untargeted and targeted methods in mass spectrometry-based metabolomics and lipidomics.* Analytical chemistry, 2016. **88**(1): p. 524-545.

155. Tsugawa, H., et al., *MRMPROBS: a data assessment and metabolite identification tool for large-scale multiple reaction monitoring based widely targeted metabolomics.* Analytical chemistry, 2013. **85**(10): p. 5191-5199.

156. Lee, H.-C. and T. Yokomizo, *Applications of mass spectrometry-based targeted and non-targeted lipidomics.* Biochemical and biophysical research communications, 2018. **504**(3): p. 576-581.

157. Lone, A.M. and K. Taskén, *Proinflammatory and immunoregulatory roles of eicosanoids in T cells.* Frontiers in immunology, 2013. **4**: p. 130.

158. Isobe, Y. and M. Arita, *Identification of novel omega-3 fatty acid-derived bioactive metabolites based on a targeted lipidomics approach.* Journal of clinical biochemistry and nutrition, 2014. **55**(2): p. 79-84.

159. Serhan, C.N., et al., *Lipid mediators in the resolution of inflammation.* Cold Spring Harbor perspectives in biology, 2015. **7**(2): p. a016311.

160. Wei, J., et al., *Derivatization strategy combined with parallel reaction monitoring for the characterization of short-chain fatty acids and their hydroxylated derivatives in mouse.* Analytica Chimica Acta, 2020. **1100**: p. 66-74.

161. Ayala, A., M.F. Muñoz, and S. Argüelles, *Lipid peroxidation: production, metabolism, and signaling mechanisms of malondialdehyde and 4-hydroxy-2-nonenal.* Oxidative medicine and cellular longevity, 2014. **2014**.

162. Vance, D.E. and J.E. Vance, *Biochemistry of lipids, lipoproteins and membranes*. Vol. 36. 2002: Elsevier.

163. Chanput, W., J.J. Mes, and H.J. Wichers, *THP-1 cell line: an in vitro cell model for immune modulation approach.* International Immunopharmacology, 2014. **23**(1): p. 37-45.

164. Dull, T., et al., *A third-generation lentivirus vector with a conditional packaging system.* Journal of Virology, 1998. **72**(11): p. 8463-8471.

165. Nishijo, J., S. Moriyama, and S. Shiota, *Interactions of cholesterol with cyclodextrins in aqueous solution.* Chemical and pharmaceutical bulletin, 2003. **51**(11): p. 1253-1257.

166. Loftsson, T., et al., *Self‐association and cyclodextrin solubilization of drugs.* Journal of pharmaceutical sciences, 2002. **91**(11): p. 2307-2316.

167. Käkelä, R., et al., *Overexpression of OSBP-related protein 2 (ORP2) in CHO cells induces alterations of phospholipid species composition.* Biochemistry and Cell Biology = Biochimie Et Biologie Cellulaire, 2005. **83**(5): p. 677-683.

168. Bauernfeind, F.G., et al., *Cutting edge: NF-κB activating pattern recognition and cytokine receptors license NLRP3 inflammasome activation by regulating NLRP3 expression.* The Journal of Immunology, 2009. **183**(2): p. 787-791.

169. Sakurada, S., T. Kato, and T. Okamoto, *Induction of cytokines and ICAM-1 by proinflammatory cytokines in primary rheumatoid synovial fibroblasts and inhibition by N-acetyl-L-cysteine and aspirin.* International Immunology, 1996. **8**(10): p. 1483-1493.

170. Montgomery, K.F., et al., *Activation of endothelial-leukocyte adhesion molecule 1 (ELAM-1) gene transcription.* Proceedings of the National Academy of Sciences, 1991. **88**(15): p. 6523-6527.

171. Devin, A., et al., *The distinct roles of TRAF2 and RIP in IKK activation by TNF-R1: TRAF2 recruits IKK to TNF-R1 while RIP mediates IKK activation.* Immunity, 2000. **12**(4): p. 419-429.

172. Hsu, H., J. Xiong, and D.V. Goeddel, *The TNF receptor 1-associated protein TRADD signals cell death and NF-kappa B activation.* Cell, 1995. **81**(4): p. 495-504.

173. Cottin, V., J.E.S. Doan, and D.W.H. Riches, *Restricted localization of the TNF receptor CD120a to lipid rafts: a novel role for the death domain.* Journal of Immunology (Baltimore, Md. : 1950), 2002. **168**(8): p. 4095-4102.

174. Veldman, R.J., et al., *A neutral sphingomyelinase resides in sphingolipid-enriched microdomains and is inhibited by the caveolin-scaffolding domain: potential implications in tumour necrosis factor signalling.* The Biochemical Journal, 2001. **355**(Pt 3): p. 859-868.

175. Pralle, A., et al., *Sphingolipid-cholesterol rafts diffuse as small entities in the plasma membrane of mammalian cells.* The Journal of Cell Biology, 2000. **148**(5).

176. Zhang, X., et al., *Cav-1 (Caveolin-1) deficiency increases autophagy in the endothelium and attenuates vascular inflammation and atherosclerosis.* Arteriosclerosis, thrombosis, and vascular biology, 2020. **40**(6): p. 1510-1522.

177. Bernatchez, P., et al., *A noninhibitory mutant of the caveolin-1 scaffolding domain enhances eNOS-derived NO synthesis and vasodilation in mice.* The Journal of clinical investigation, 2011. **121**(9).

178. Ramírez, C.M., et al., *Caveolin-1 regulates atherogenesis by attenuating low-density lipoprotein transcytosis and vascular inflammation independently of endothelial nitric oxide synthase activation.* Circulation, 2019. **140**(3): p. 225-239.

179. Fernández-Hernando, C., et al., *Endothelial-specific overexpression of caveolin-1 accelerates atherosclerosis in apolipoprotein E-deficient mice.* The American journal of pathology, 2010. **177**(2): p. 998-1003.

180. Yamamoto, K., et al., *Shear stress activates mitochondrial oxidative phosphorylation by reducing plasma membrane cholesterol in vascular endothelial cells.* Proceedings of the National Academy of Sciences, 2020. **117**(52): p. 33660-33667.

181. Payne, S., S. De Val, and A. Neal, *Endothelial-Specific Cre Mouse Models.* Arteriosclerosis, Thrombosis, and Vascular Biology, 2018. **38**(11): p. 2550-2561.

182. Venable, M.E., et al., *Role of ceramide in cellular senescence.* The Journal of Biological Chemistry, 1995. **270**(51): p. 30701-30708.

183. Venable, M.E. and X. Yin, *Ceramide induces endothelial cell senescence.* Cell Biochemistry and Function, 2009. **27**(8): p. 547-551.

184. Slotte, J.P., *Biological functions of sphingomyelins.* Progress In Lipid Research, 2013. **52**(4): p. 424-437.

185. Galvagnion, C., et al., *Sphingolipid changes in Parkinson L444P GBA mutation fibroblasts promote α-synuclein aggregation.* Brain : a Journal of Neurology, 2022. **145**(3): p. 1038-1051.

186. Dehghan, A., et al., *Metabolome-wide association study on ABCA7 indicates a role of ceramide metabolism in Alzheimer's disease.* Proceedings of the National Academy of Sciences of the United States of America, 2022. **119**(43): p. e2206083119.

187. Lemay, A.-M., et al., *High FA2H and UGT8 transcript levels predict hydroxylated hexosylceramide accumulation in lung adenocarcinoma.* Journal of Lipid Research, 2019. **60**(10): p. 1776-1786.

188. Lidgard, B., et al., *High-Density Lipoprotein Lipidomics in Chronic Kidney Disease.* Clinical Chemistry, 2023. **69**(3): p. 273-282.

189. Xie, D., et al., *Distinct effects of different phosphatidylglycerol species on mouse keratinocyte proliferation.* PLoS One, 2014. **9**(9): p. e107119.

190. McCarthy, C.G., et al., *Toll-like receptors and damage-associated molecular patterns: novel links between inflammation and hypertension.* American Journal of Physiology-Heart and Circulatory Physiology, 2014. **306**(2): p. H184-H196.

191. Kuronuma, K., et al., *Anionic Pulmonary Surfactant Phospholipids Inhibit Inflammatory Responses from Alveolar Macrophages and U937 Cells by Binding the Lipopolysaccharide-interacting Proteins CD14 and MD-2**. Journal of Biological Chemistry, 2009. **284**(38): p. 25488-25500.

192. Kandasamy, P., et al., *Pulmonary surfactant phosphatidylglycerol inhibits Mycoplasma pneumoniae-stimulated eicosanoid production from human and mouse macrophages.* Journal of Biological Chemistry, 2011. **286**(10): p. 7841-7853.

193. Naguib, A., et al., *p53 mutations change phosphatidylinositol acyl chain composition.* Cell reports, 2015. **10**(1): p. 8-19.

194. Brites, P., H.R. Waterham, and R.J.A. Wanders, *Functions and biosynthesis of plasmalogens in health and disease.* Biochimica Et Biophysica Acta, 2004. **1636**(2-3): p. 219-231.

195. Broniec, A., et al., *Interactions of plasmalogens and their diacyl analogs with singlet oxygen in selected model systems.* Free Radical Biology & Medicine, 2011. **50**(7): p. 892-898.

196. Benjamin, D.I., et al., *Ether lipid generating enzyme AGPS alters the balance of structural and signaling lipids to fuel cancer pathogenicity.* Proceedings of the National Academy of Sciences of the United States of America, 2013. **110**(37): p. 14912-14917.

197. Li, X., et al., *Lysophospholipids induce innate immune transdifferentiation of endothelial cells, resulting in prolonged endothelial activation.* Journal of Biological Chemistry, 2018. **293**(28): p. 11033-11045.

198. Semba, R.D., et al., *Low plasma lysophosphatidylcholines are associated with impaired mitochondrial oxidative capacity in adults in the Baltimore Longitudinal Study of Aging.* Aging Cell, 2019. **18**(2): p. e12915.

199. Mapstone, M., et al., *Plasma phospholipids identify antecedent memory impairment in older adults.* Nature Medicine, 2014. **20**(4): p. 415-418.

200. Gonzalez-Freire, M., et al., *Targeted Metabolomics Shows Low Plasma Lysophosphatidylcholine 18:2 Predicts Greater Decline of Gait Speed in Older Adults: The Baltimore Longitudinal Study of Aging.* The Journals of Gerontology. Series A, Biological Sciences and Medical Sciences, 2019. **74**(1): p. 62-67.

201. Lee, S.Y., et al., *Lysophosphatidylglycerol stimulates chemotactic migration and tube formation in human umbilical vein endothelial cells.* Biochemical and Biophysical Research Communications, 2007. **363**(3): p. 490-494.

202. Martin, T.W. and D. Lagunoff, *Interactions of lysophospholipids and mast cells.* Nature, 1979. **279**(5710): p. 250-252.

203. Xu, Y., G. Casey, and G.B. Mills, *Effect of lysophospholipids on signaling in the human Jurkat T cell line.* Journal of Cellular Physiology, 1995. **163**(3): p. 441-450.

204. Inoue, A., et al., *TGFα shedding assay: an accurate and versatile method for detecting GPCR activation.* Nature Methods, 2012. **9**(10): p. 1021-1029.

205. Wiley, C.D., et al., *Oxylipin biosynthesis reinforces cellular senescence and allows detection of senolysis.* Cell Metabolism, 2021. **33**(6).

206. Lizardo, D.Y., et al., *Regulation of lipids is central to replicative senescence.* Molecular BioSystems, 2017. **13**(3): p. 498-509.

207. Wiley, C.D., et al., *Secretion of leukotrienes by senescent lung fibroblasts promotes pulmonary fibrosis.* JCI Insight, 2019. **4**(24).

208. Biran, A., et al., *Quantitative identification of senescent cells in aging and disease.* Aging cell, 2017. **16**(4): p. 661-671.

209. Beck, J., I. Horikawa, and C. Harris, *Cellular senescence: mechanisms, morphology, and mouse models.* Veterinary Pathology, 2020. **57**(6): p. 747-757.

210. Herranz, N. and J. Gil, *Mechanisms and functions of cellular senescence.* The Journal of clinical investigation, 2018. **128**(4): p. 1238-1246.

211. Kuilman, T., et al., *The essence of senescence.* Genes & development, 2010. **24**(22): p. 2463-2479.

212. McMahon, H.T. and J.L. Gallop, *Membrane curvature and mechanisms of dynamic cell membrane remodelling.* Nature, 2005. **438**(7068): p. 590-596.